

University of Hradec Králové  
Faculty of Informatics and Management  
Department of Informatics

**Optimization the Power Output of Solar Panel Using Smart Hardware  
Case Study about Dual Access Solar Tracker**

**BACHELOR'S THESIS**

Author: Mina Bayat

Branch of study: Information Management

Advisor: Ing. Jan Štěpán

2017 Hradec Králové

## **Declaration**

I declare I wrote the Bachelor's thesis "Optimization the Power Output of Solar Panel Using Smart Hardware" myself, using only the listed bibliography.

The research was done under the support and guidance of Ing. Jan Štěpán

In Hradec Králové.

Date:.....

Signature:.....

## **Dedication**

I wish to dedicate this thesis to my parents who always taught me the greatest lessons, not only by their hard work and dedication, but also through their kind and sincere actions toward anyone regardless of all the barriers that separate people.

I wish to also include all those beloved ones who held my hand in times of desperation, brightened my heart in times of despair and calmed my mind in times of fear, giving me the courage and hope to keep going.

I could not write this thesis today, nor had I the chance to come this far, if it was not for them all; for their support, for their love and their faith in me, regardless of all my flaws and failures.

## **Acknowledgements**

I wish to express my sincere thanks to my supervisor Ing. Jan Štěpán. I am extremely thankful and indebted to him for sharing expertise, valuable guidance, patience and encouragement extended to me.

I would also wish to sincerely thank professor doc. RNDr. Jaroslava Mikulecká, CSc., professor doc. RNDr. Tatiana Gavalcová, CSc. and professor RNDr. Peter Mikulecký, Ph.D. for their kind care and assistance to me especially at the beginning of my studies.

I wish to truthfully thank all my teachers who kindly and patiently helped me throughout this challenging yet interesting journey.

Finally, I take the opportunity to express my gratitude to all of the department and faculty members, and the university staff for their kind help and support including Ing. Vendula Pourová, who never hesitated to help me any time I needed her assistance and insight.

## **Abstract**

Solar panels are one of the popular energy convertors. This thesis focuses on the achievement of optimized output from the solar panel by controlling its position with regard to the position of sun in the sky, with the use of smart hardware and photoresistors.

For this purpose a prototype is designed and built that consists of the housing structure for the solar panel providing the possibility for the solar panel to track the sun and rotate accordingly by stepper motors, a microcontroller board and necessary commands and instructions in form of a program code usable by the microcontroller board.

The prototype was tested versus a fixed solar panel and proved the efficiency of output voltage in dual-axis tracker, and the results proved theoretical background to be right.

## **Abstrakt**

Solární panely jsou jedním z oblíbených konvertorů energie. Tato kvalifikační práce se zaměřuje na dosažení optimalizovaného výstupu ze solárního panelu ovládním jeho polohy s ohledem na postavení slunce na obloze, při použití chytrého hardware a fotorezistorů.

K tomuto účelu byl navržen a postaven prototyp, který sestává ze stojanu poskytujícího oporu pro solární panel tak, aby mohl sledovat pohyb slunce a otáčet se odpovídajícím způsobem pomocí krokových elektromotorů, desky mikrořadiče a nezbytných příkazů a instrukcí ve formě kódu programu použitého pro desku mikrořadiče.

Prototyp byl testován na pevném solárním panelu a byla dokázána efektivnost výstupního napětí v dvouosém sledovači a výsledky dokázaly správnost teoretického pozadí.

# Table of Contents

<b>1. Introduction</b> .....	1
<b>2. Literature review</b> .....	2
2.1 Photovoltaic System.....	2
2.1.1 Sun and Nature of Light Energy .....	2
2.1.2 Solar Radiation on Sloped Surface .....	4
2.1.3 One-Axis Tracking Flat-Plate Collectors with Axis Oriented North-South.....	8
2.1.4 Dual-Axis Tracking Flat-Plate Collectors .....	9
2.1.5 Effective Heat Collection Concept .....	10
2.1.6 Studies related to Output Optimization Relating to Slope.....	11
2.1.7 Shading .....	12
2.1.8 PV Cell.....	12
2.2 Motors .....	13
2.2.1 External Structure .....	13
2.2.2 Internal Structure .....	14
2.2.3 Choosing the Right Motor .....	15
2.2.4 DC Motors Fundamentals .....	16
2.2.5 Stepper Motors.....	17
2.2.6 Permanent Magnet (PM) Steppers .....	18
2.2.7 Variable-reluctance (VR).....	19
2.2.8 Hybrid (HY) Steppers .....	20
2.2.9 Bipolar Stepper Control .....	21
2.2.10 Unipolar Stepper Control.....	22
2.2.11 Servo Motors.....	25
<b>3. Main Chapters</b> .....	28

3.1 Practical Approach.....	28
3.1.1 Solar Panel Supporting Structure.....	28
3.1.2 Motors.....	31
3.1.3 Tracking System.....	31
3.2 Testing.....	36
3.3 Economical Approach.....	37
<b>4. Results.....</b>	<b>40</b>
<b>5. Conclusions and Recommendations.....</b>	<b>41</b>
<b>Bibliography.....</b>	<b>42</b>
<b>Appendix.....</b>	<b>46</b>
Appendix 1.....	46
Appendix 2.....	47
Appendix 3.....	48
Appendix 4.....	49

## List of Figures

Figure 1: Earth's atmosphere's effect on sun's light reaching the surface of earth .....	3
Figure 2: Two-dimensional illustration of effect of collector tilt on effective area.....	4
Figure 3: Relationships among $\theta$ , $\delta$ and $\phi$ at solar noon in winter and summer .....	5
Figure 4: Cumulative daily irradiation received by fixed and tracking collectors .....	6
Figure 5: Optimizing the mounting angle of a fixed collector.....	7
Figure 6: One-axis tracking flat-plate collector with axis oriented north-south.....	9
Figure 7: Dual-axis tracking flat-plate collector .....	9
Figure 8: Energy balance schematic drawing of a solar collector .....	10
Figure 9: Cells, modules and arrays.....	13
Figure 10: A simple electric motor .....	14
Figure 11: Internal structure of an electric motor .....	15
Figure 12: Motor selection flowchart .....	16
Figure 13: A permanent magnet (PM) stepper motor .....	18
Figure 14: Principle of a PM or tin-can stepper motor .....	19
Figure 15: Cross-section of a variable-reluctance (VR) motor.....	20
Figure 16: A hybrid (HY) stepper.....	21
Figure 17: Connections of a bipolar stepper motor .....	21
Figure 18: Controlling one phase of a bipolar stepper with an H bridge.....	22
Figure 19: Electromagnet circuits with a center tap .....	23
Figure 20: Connections of a unipolar stepper .....	24
Figure 21: Sample wiring diagrams in a stepper datasheet.....	25
Figure 22: The FS5106B servomotor from Fitec.....	26
Figure 23: Closed-loop angular position control using DC motor .....	26
Figure 24: Worm and wheel gears .....	30

Figure 25: Solar panel supporting structure.....	30
Figure 26: Breadboard view of the designed prototype circuit.....	33
Figure 27: Schematic view of the designed prototype circuit.....	34

## List of Tables

Table 1: Output voltage of solar panel mounted on the prototype and the fixed solar panel ...	37
Table 2: Selected properties of 300W Outdoor Stand Alone Solar Panel .....	38
Table 3: Total energy received and totals costs for dual-axis and fixed methods .....	39
Table 4: Total energy recieved for dual-axis and fixed methods based the testing result .....	40

## List of Equations

Equation 1: Relationships among $\theta$ , $\delta$ and $\phi$ at solar noon in winter and summer.....	5
Equation 2: Efficiency of the solar collector .....	10
Equation 3: Torque produced by a DC motor.....	17
Equation 4: Voltage loss by motor's armature's resistance.....	17
Equation 5: Conversion of motor's input voltage and input current to torque and speed .....	17

## 1. Introduction

Energy is one of the major concerns all over the world today. Due to the problems and threats that concern non-renewable sources of energy such as coal, crude oil and uranium as fuel for nuclear power plants, a migration toward clean sources of energy has already started. This movement has resulted in more studies and attempts toward improvements of clean energy production technologies including solar panels.

Solar energy is free and available for many areas on the earth almost all through the year. These properties make it one of the most popular and affordable clean energy. However, since the position of the sun in the sky is constantly changing, especially for areas where receive fewer amounts of sun rays on the surface, it is important that solar panels receive the solar energy as much as possible throughout the time that the sun is in the sky. One way to achieve this goal is for the solar panel to track the location of the sun in the sky.

This method can become feasible with the help of smart hardware. This research consists of three parts. The first part concerns the theoretical knowledge regarding solar energy, methods of its collection and optimization, and DC and stepper motors.

In the second part the method of solar energy collection and based on that the designed smart hardware are introduced and explained. Lastly, in the third part the collected data from two solar panels' output and based on that a computation is done to determine the profitability of the dual-axis tracking over fixed method. One of the solar panels is capable of tracking the sun with the use of the designed smart hardware and the other solar panel has simply a fixed horizontal position. The observation and collection of data from two solar panels are done under the same environmental conditions.

## **2. Literature review**

In this part the current information regarding photovoltaic systems in general, the regarding principles, different manner of collecting and motors, more precisely DC motors are briefly reviewed.

### **2.1 Photovoltaic System**

Photovoltaic systems are power systems that react to light by transforming part of it into electricity. Photovoltaic systems have properties that make them novel and unique including having no moving parts wear out, containing no fluid or thermal gases (except in hybrid systems) that can leak out, having rapid response, being able to operate at moderate temperatures and so many other, producing no pollution while operating and being able to be made from silicon, the second most abundant element in the earth's crust. (Solar Energy Research Institute, 1982)

#### **2.1.1 Sun and Nature of Light Energy**

It is important to know properties of sunlight since optimization of the performance of photovoltaic and other systems that convert sunlight into other useful forms of energy is based on this knowledge. (Messenger & Ventre, 2004)

The sun, while producing X-Ray and other energies, releases 95% of its output energy as light, some of which cannot be seen by the human eye. (Solar Energy Research Institute, 1982)

When sunlight enters the Earth's atmosphere some of it is absorbed to the atmosphere while some is scattered and some other passes through atmosphere unaffected by the molecules there or finally get absorbed or reflected by objects on the surface of earth. (Messenger & Ventre, 2004)

It is important to consider the relation between the amount of sunlight at the Earth's surface and the quantity, or air mass (AM), of atmosphere through which the light must pass. Radiation arriving at the surface of the earth is measured against the radiation that reaching the borders of the atmosphere where there is no air, and therefore, the air mass is zero (AM0). (Solar Energy Research Institute, 1982)

The atmosphere is a powerful sunlight energy absorber and can cut the sun's energy reaching the earth by 50% and more. As a result, the intensity of the sunlight reaching the ground weakens for sun angles approaching the horizon, or for the air mass that it has to penetrate. (Dunlop, 2009)

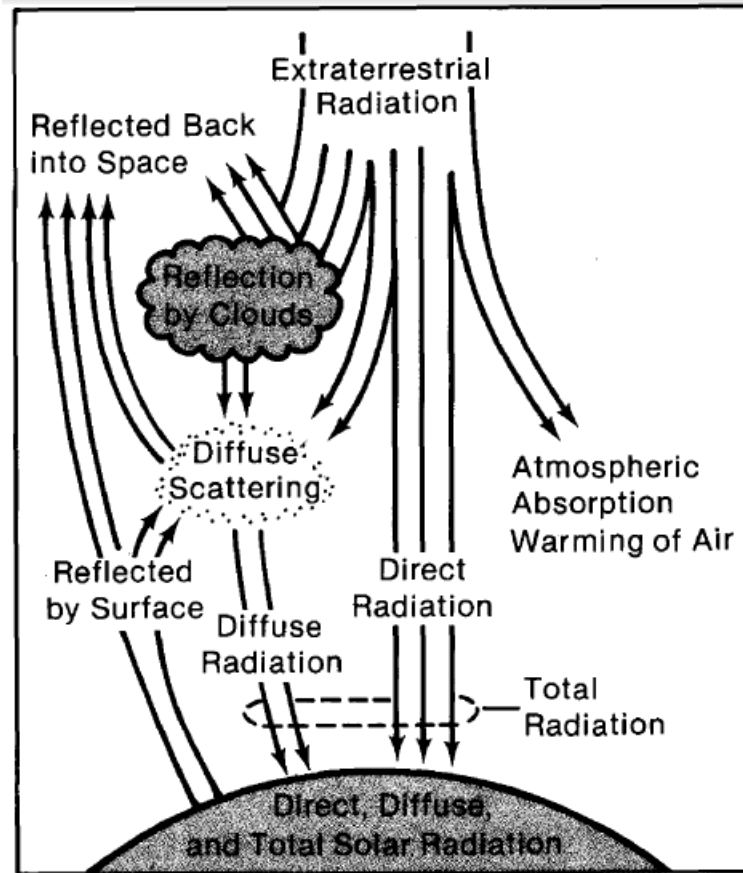


Figure 1 – The earth's atmosphere and clouds affect the way in which the sun's light reaches the surface of the earth. Source: (Solar Energy Research Institute, 1982)

The power density of sunlight is measured as Irradiance in  $W/m^2$ . Therefore, Irradiance is an instantaneous quantity. The irradiance which is received by the Earth from the sun at the top of the atmosphere (at AM0) is the solar constant for Earth which is equal to  $1367 \text{ } W/m^2$ . (Messenger & Ventre, 2004)

The energy density of sunlight is measured as Irradiation in  $kWh/m^2$ . As expected Irradiation is the integral of irradiance Since energy is power that is integrated over time. Usually the time frame for integration is one day which means during daylight hours. (Sukhatme & Sukhatme, 1996)

## 2.1.2 Solar Radiation on Sloped Surface

Designing a mounting for a system that collects sunlight is important for it can influence the outcome of the system considerably. It may appear that the easiest manner of mounting of most systems is to mount them horizontally. However, this direction does not optimize collection. According to Messenger & Ventre (2004) that is because the beam radiation component collected is proportional to the cosine of the angle between the incident beam and the normal to the plane of the collector, as shown in figure 2.

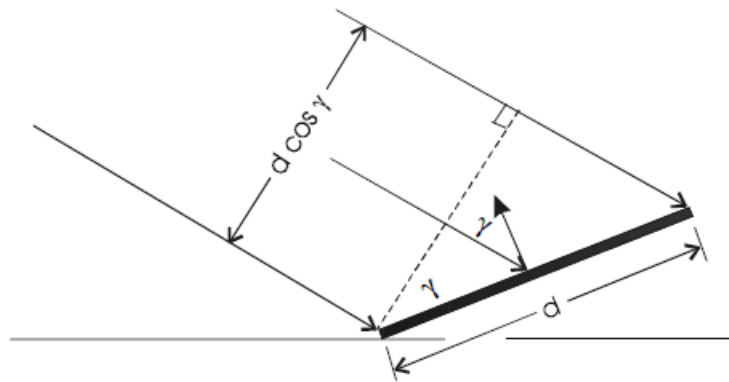


Figure 2 – Two-dimensional illustration of effect of collector tilt on effective area presented to beam component of radiation. Source: (Messenger & Ventre, 2004)

Depending on the ratio of diffuse to beam irradiance components, the portion of available energy that is received will be between  $\cos \gamma$ , and unity. Equation 1 shows that if a collector is mounted with its plane perpendicular to zenith angle ( $\theta_z$ ) at solar noon, it will be perpendicular to the sun at solar noon. This is the point at which the sun is highest in the sky that results in its minimum path through the atmosphere and corresponding lowest air mass for the day. (Messenger & Ventre, 2004)

The zenith is a line perpendicular to the Earth that is straight up. The zenith angle ( $\theta_z$ ) is defined as the angle between the sun and the zenith. The tendency can be related to the zenith angle at solar noon by noting that the sun is at its highest point in the sky at solar noon. Since the sun travels through an angle of  $15^\circ$  per hour, it will be close to perpendicular to the collector for a

period of approximately two hours. Beyond this time, the intensity of the sunlight decreases due to the increase in air mass, and the angle between incident sunlight and the normal to the collector increases. These two factors cause the energy collected by the collector to decrease comparatively rapidly during the hours before 10 a.m. and after 2 p.m. (Sukhatme & Sukhatme, 1996)

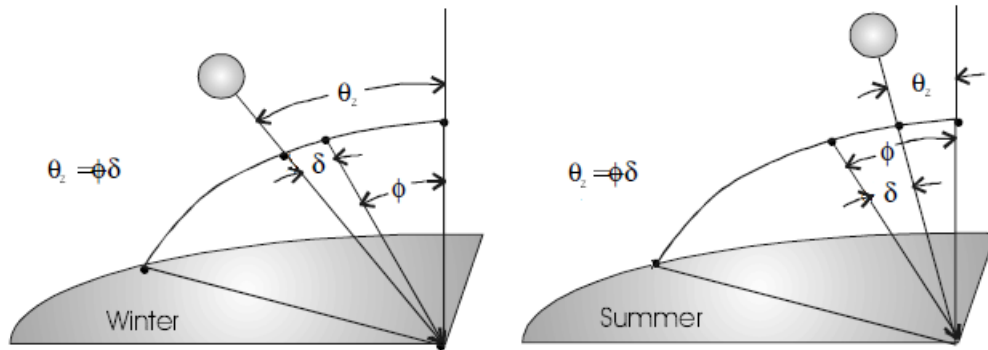


Figure 3 – Relationships among  $\theta_z$ ,  $\delta$  and  $\phi$  at solar noon in winter and summer. Source: (Messenger & Ventre, 2004)

Equation 1:  $\theta_z = \phi - \delta$

Figure 4 show the approximate cumulative irradiation received by a south-facing collector sloped at the latitude angle in a region where the beam radiation component is significantly stronger than either the diffuse or the albedo components. If the collector is mounted in a way that allows it to track the sun, then the incident irradiance is affected only by the increasing air mass as the sun approaches the horizon. The figure also shows the additional cumulative irradiation under direct beam condition received by a tracking collector. Approximately 50% more energy can be collected in the summer in a dry climate (such as that found in Phoenix in Arizona) by using a tracking collector. During winter months, however, only about 20% more energy is collected using a tracker. (Dunlop, 2009)

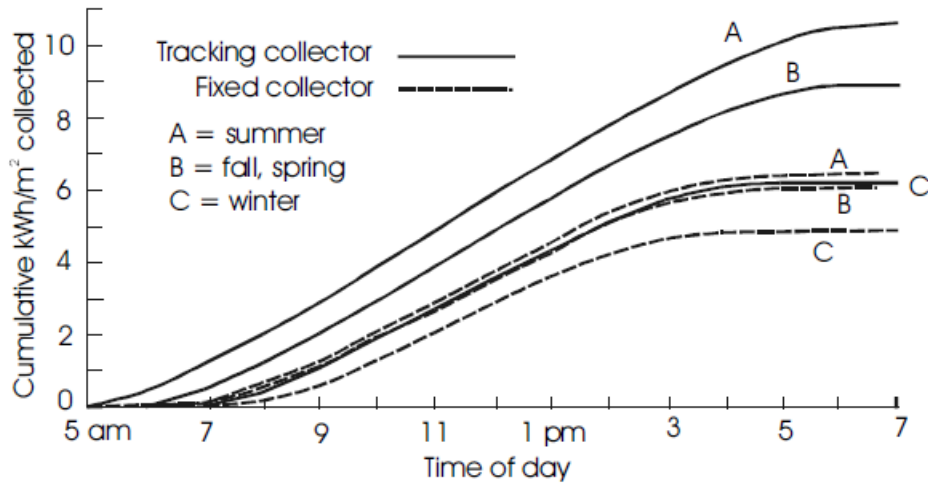


Figure 4 – Cumulative daily irradiation received by fixed and tracking collectors for different seasons, direct beam contribution only. Source: (Messenger & Ventre, 2004)

For mounting selection, a single-axis tracker can be considered which rotates about an axis fixed with respect to  $\theta_z$ . It can then be also considered mountings that can be adjusted manually several times per day or, perhaps, several times per year. Each of these options will enable the collection of an amount of energy that lies somewhere between the optimized fixed collector and the dual-axis tracking collector results. (Messenger & Ventre, 2004)

Collector orientation may also depend on the season. For example, a remote cabin that is used only during summer months will require its collector oriented for optimal summer collection. However, if the cabin is used in the winter as a ski lodge, or in the fall as a hunting base, then the collector may need to be optimized for one of these seasons. (Sukhatme & Sukhatme, 1996)

According to Messenger and Ventre (2004) for optimal performance on any given day, a fixed collector should be mounted with its plane at an angle of  $\phi - \delta$  with regard to the horizontal, as it is demonstrated in figure 5. This will cause the plane of the collector to be perpendicular to the sun at solar noon.

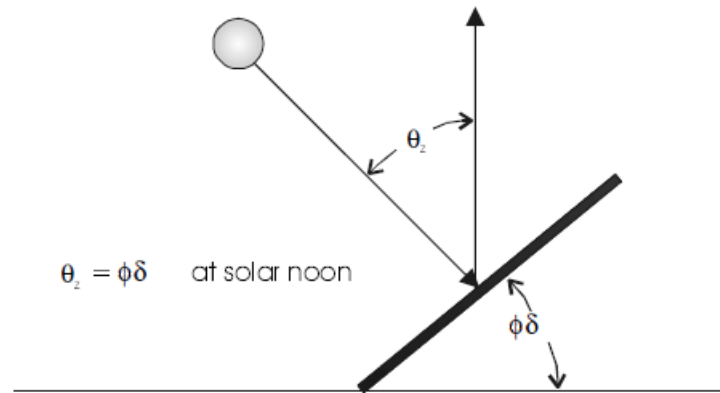


Figure 5 – Optimizing the mounting angle of a fixed collector. Source: (Messenger & Ventre, 2004)

For optimal seasonal performance, then, one simply chooses the average value of  $\delta$  for the season. Knowing  $\delta$  variations for summer in northern hemisphere for each month, and also knowing that the average value of half a sine wave having amplitude  $A$ , is  $2A/\pi$ ; it is then possible to calculate average declination for each month. Therefore, it can be driven that the average declination between March 21 and September 21 is  $14.93^\circ$ . In a similar manner, the average declination for the period from September 21 to March 21 is  $-14.93^\circ$ . Hence, for best average summer performance, a collector should be mounted at approximately  $\phi - 15^\circ$ , and for best average winter performance, it should be mounted at  $\phi + 15^\circ$ . Lastly, for optimum spring or fall performance or optimum annual performance, the collector should be mounted at about  $0.9\phi^\circ$ . (Messenger & Ventre, 2004)

Since normally it is acceptable to orient a collector for optimal seasonal or, perhaps, annual performance, many tables of irradiation on collectors are available for collector slopes of either  $\phi$ ,  $\phi + 15^\circ$  or  $\phi - 15^\circ$  at various locations on the globe. (Dunlop, 2009)

Stanciu & Stanciu (2014) estimated solar radiation density based on three analysis models in order to find optimum slope angle for flat plate collectors at different geographical locations and different time moments over a year. The absorbed solar radiation density was computed and the optimum tilt angle was found for different geographical locations (covering the Globe latitudes).

The optimum value for the slope angle was researched for maximum incident solar radiation and also for maximum absorbed one.

The three analysis models used in the study were as follows: Hottel and Woertz model (the simplest), Isotropic diffuse model (Liu & Jordan model) and HDKR model (Hay–Davis–Klucker–Reindl), with the later being the most complex one. The results detected that the same angle is obtained when looking for maximum incident and for maximum absorbed solar radiation. (Stanciu & Stanciu, 2014)

The results also indicated that when using the Hottel & Woertz model for estimating the incident solar radiation, the optimum tilt angle for a flat plate collector should be computed as simplest as  $\beta_{opt} = \phi - \delta$  function on the latitude and solar declination. However, when either isotropic or anisotropic diffuse models are applied, the previous values should be changed by  $+10^\circ$ . (Stanciu & Stanciu, 2014)

### **2.1.3 One-Axis Tracking Flat-Plate Collectors with Axis Oriented North-South**

Data are presented for four different axis slope angles from the horizontal:  $0^\circ$ , latitude minus  $15^\circ$ , latitude, and latitude plus  $15^\circ$ . These trackers pivot on their single axis to track the sun facing east in the morning and west in the afternoon. Large collectors can use an axis slope angle of  $0^\circ$  to minimize collector height and wind force. Small collectors can have their axis sloped up to increase the solar radiation on the collector. Just as for the flat-plate fixed tilt collector, the yearly and seasonal solar radiation can be optimized by the choice of tilt angle. The data presented assume continuous tracking of the sun throughout the day. (Marion & Wilcox, 1994)

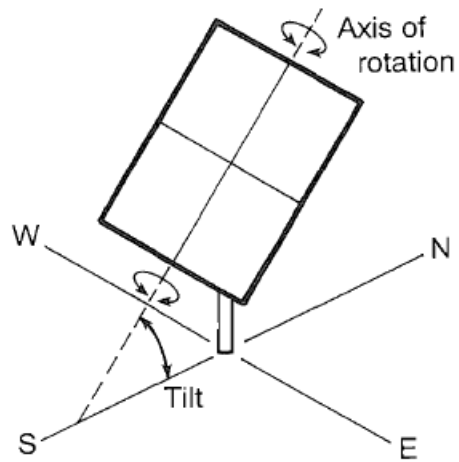


Figure 6 – One-axis tracking flat-plate collector with axis oriented north-south. Source: (Marion & Wilcox, 1994)

### 2.1.4 Dual-Axis Tracking Flat-Plate Collectors

Data for dual-axis trackers demonstrates the maximum solar radiation at a site available to a collector. Tracking the sun in both azimuth and elevation, these collectors keep the sun's rays normal to the collector surface. (Marion & Wilcox, 1994)

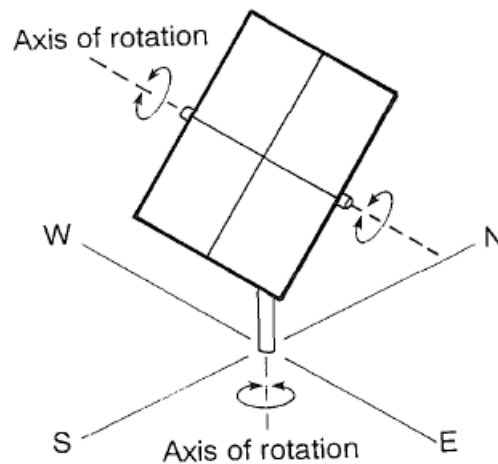


Figure 7 – Dual-axis tracking flat-plate collector. Source: (Marion & Wilcox, 1994)

## 2.1.5 Effective Heat Collection Concept

Available or effective heat received by the collector within a certain period is the energy difference between the captured solar energy and the energy lost to ambient environment, in which absorbed solar energy is the solar energy reaching the collector surface subtracted by thermal loss due to collector radiation. (Sukhatme & Sukhatme, 1996)

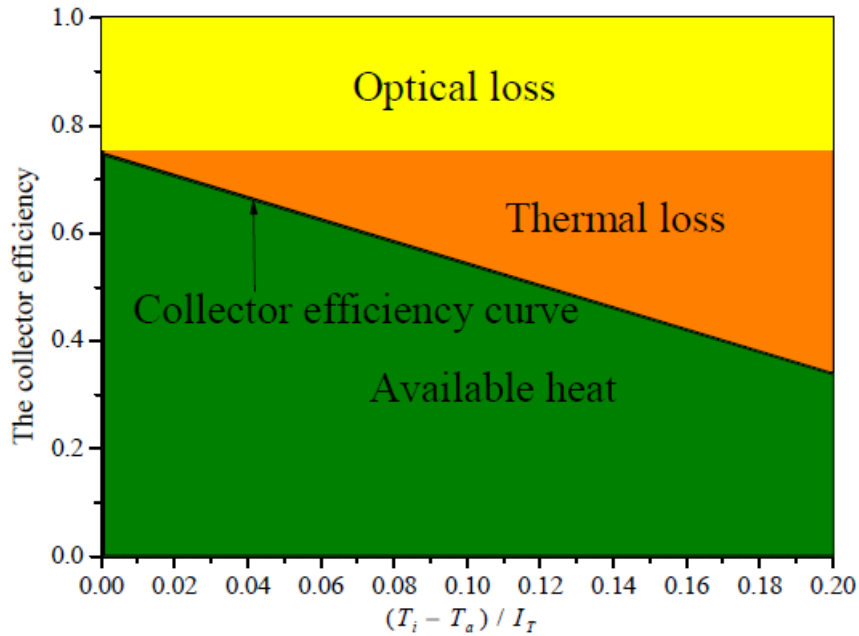


Figure 8 – Energy balance schematic drawing of a solar collector. Source: (Lv, et al., 2016)

The following equation is applicable for most collectors:

$$\text{Equation 2: } \eta = Q_u / A I_T = F_R (\tau\alpha)_n - F_R U_L (T_i - T_a) / I_T$$

Lv, et al., (2016) explains that where  $\eta$  is the efficiency of the solar collector;  $Q_u$  is the output energy from the collector, in Watt;  $A$  is the solar collector surface, in  $m^2$ ;  $I_T$  is the solar irradiance received per collector area, in  $W/m^2$ ;  $F_R$  is the collector efficiency factor;  $(\tau\alpha)_n$  is the effective transmittance-absorptance product at normal incidence;  $U_L$  is the overall heat loss

coefficient, in  $W/(C^\circ \cdot m^2)$ ;  $T_i$  is the mean fluid temperature through solar field, in  $C^\circ$ ;  $T_a$  is the ambient air temperature, in  $C^\circ$ .

When solar collector efficiency  $\eta = 0$ ,  $[(T_i - T_a)/I_T]c$  is defined as critical normalization temperature at which the absorbed solar energy equals to heat loss. In case of  $[(T_i - T_a)/I_T]t < [(T_i - T_a)/I_T]c$ ,  $\eta > 0$  the collector could obtain effective heat when the solar radiation energy absorbed by the collector is greater than the collector energy lost to ambient environment. Contrariwise, the collector would dissipate heat to the ambient environment. Therefore, the effective heat collection of solar collector system can be defined as the energy difference between the absorbed solar irradiance and the collector energy radiated to ambient environment when the normalization temperature at time  $t$  is lower than the critical normalization temperature. (Lv, et al., 2016)

### **2.1.6 Studies related to Output Optimization Relating to Slope**

Despite of practicality and popularity of the method mentioned above, research is still going on to find improved means and optimized models and methods of collecting.

As an example, in the developed model that was applied in a case study of the Lhasa district, the concept of effective heat collection was proposed and an optimized mathematical model was further developed to define the optimum slope angle and orientation for the solar collector. In the research it was concluded that the optimum installation of solar thermal collector based on effective heat collecting capacity can eliminate the ineffective solar radiation falling on the solar collector, which could determine the optimum azimuth angle and tilt angle of solar collector more accurately, to be beneficial for improving the solar thermal system efficiency. (Lv, et al., 2016)

According to Lv, et al., (2016) the case study in Lhasa showed that there is about  $5^\circ$  deviation between the optimum results acquired according to effective heat collecting capacity and the optimum results obtained according to maximum total solar radiation falling on the solar collector.

In another study by Ertekin, et al., (2008) optimal slope angles were measured for solar collectors based on the monthly global and diffuse solar radiation on a horizontal surface across Turkey. During this study, the dataset of monthly average daily global solar radiation was obtained from 158 places, and monthly diffuse radiation data were estimated using an empirical model by Tasdemiroglu and Sever.

It was concluded that the optimum slope angles exhibit a strong seasonal trend with respect to the amount of maximum daily insolation incident on the collector surface. Monthly average optimum slope angles were reasonably well estimated as a sinusoidal function of latitude and the day of the year over Turkey. Finally, it was realized that the spatially interpolated surfaces may guide the choice of annually optimal tilt angles for the fixed south-facing solar collectors, especially where there is no information about solar radiation across Turkey. (Ertekin, et al., 2008)

### **2.1.7 Shading**

It is important to avoid any shade on the PV module since it can significantly reduce the module output current. Therefore, it is advisable to select a site for a PV system where the PV array will remain unshaded for as much of the day as possible. (Dunlop, 2009)

### **2.1.8 PV Cell**

Photovoltaic systems are designed based on the photovoltaic cell. Since a typical photovoltaic cell produces less than 3 watts at approximately 0.5 volt dc, cells ought to be connected in series-parallel configurations to produce enough power for high-power applications. (Messenger & Ventre, 2004)

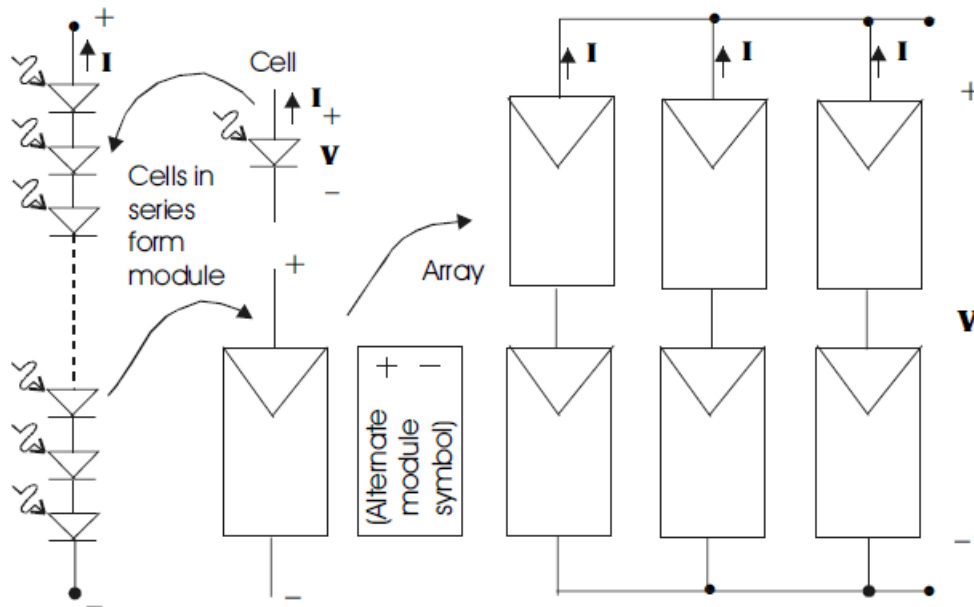


Figure 9 – Cells, modules and arrays. Source: (Messenger & Ventre, 2004)

## 2.2 Motors

Nearly every mechanical movement that is seen in machines is accomplished by an electric motor. Motors receive electrical energy and produce mechanical energy. Electric motors are in general classified into two different categories: DC (Direct Current) and AC (Alternating Current). Within these categories there are numerous types, each offering special abilities that suit them well for specific applications. DC motors are differentiated by their ability to operate from direct current. (Chen, n.d.)

### 2.2.1 External Structure

The externals of an electrical motor include:

- ❖ Case or shell - The external casing that envelops the motor
- ❖ Shaft - The metal cylinder that outstretches from the motor's center

- ❖ Wires or leads - The conductors that transport electricity to the motor

The electrical input is delivered to the motor through the leads. As the motor functions, it rotates the shaft. This shaft is usually connected to a load. (Kirtley & Beaty, 1998)



Figure 10 – A simple electric motor. Source: (Scarpino, 2015)

### 2.2.2 Internal Structure

According to Scarpino (2015) a motor's structure can be perceived in two ways, mechanically and electrically. From a mechanical point of view, the motor consists of two parts; the rotor, that is the part that moves; and the stator, which is the part that stays in place. The hollow space separating the rotor and stator is called the air gap.

From an electrical point of view, a motor's structure can be divided into other two parts; the armature, the part that receives current; the other part responsible for generating the magnetic field. Figure 11 displays a cross-section of a rotary motor, as current enters the motor, the central element rotates inside the case. (Scarpino, 2015)

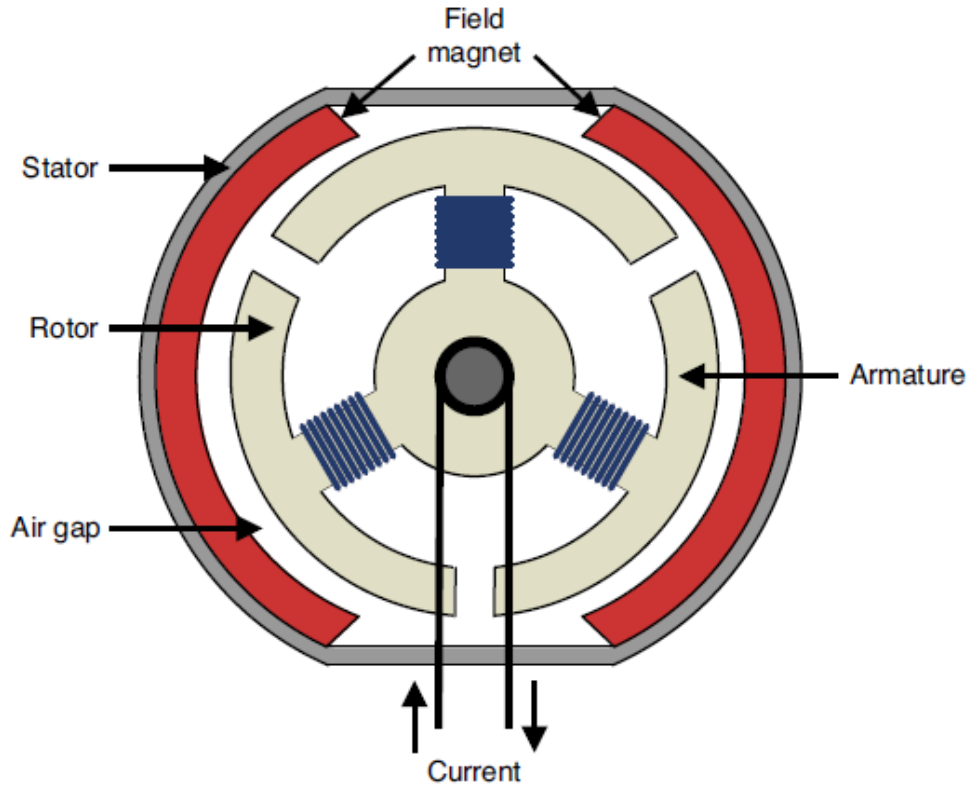


Figure 11 – Internal structure of an electric motor. Source: (Scarpino, 2015)

### 2.2.3 Choosing the Right Motor

Nowadays there are a wide range of categories and subcategories for electric motors, to choose from.

Figure 12 displays a basic decision-making process that can be used to select a appropriate motor for a particular task. The diagram can help making an initial evaluation; however, it is not a thorough breakdown of the many categories of electric motors. Not to mention, some motors do not fit into the decision-making method in the diagram. (Scarpino, 2015)

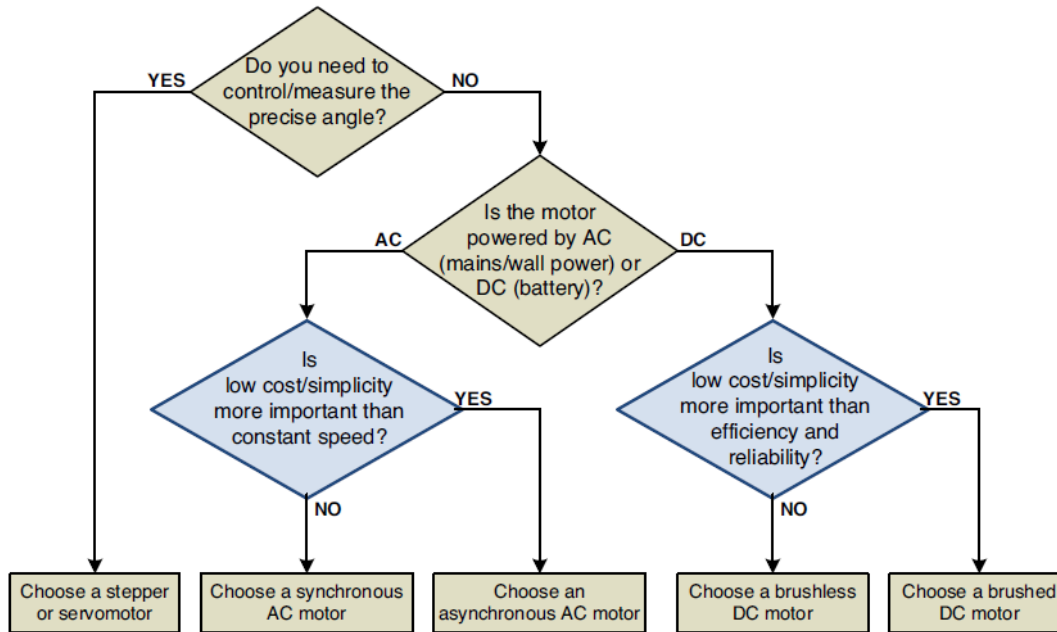


Figure 12 – Motor selection flowchart. Source: (Scarpino, 2015)

## 2.2.4 DC Motors Fundamentals

Despite of different internal structures and different methods of control in brushed and brushless DC motors, they share four characteristics in common: (Kirtley & Beaty, 1998)

- ❖ Torque is nearly proportional to current.
- ❖ Speed is nearly proportional to voltage.
- ❖ Control circuitry use electrical switches to deliver power to the motor.
- ❖ A controller can control the motor's operation using PWM (pulse width modulation) signals.

Scarpino (2015) explains that for DC motors, the relationship between torque and current can be approximated with a straight line. This means that the ratio between torque and current is generally constant. This constant is referred to as  $K_T$ . Therefore, with the current entering the armature of a motor increases, the motor's torque increases as well.

According to Scarpino (2015) when a motor's shaft rotates but exerts no torque, it is in the no-load condition. The current absorbed by a motor in its no-load condition is called the no-load

current, denoted as  $I_0$ .  $I_0$  is the minimum amount of current required to put the motor in motion. Therefore, if the motor's armature receives a current of  $I$ , the torque produced by the motor equals  $K_T(I - I_0)$ . If the torque denoted as  $\tau$  is given in N-m and  $K_T$  is given in oz-in, the equation is as follows:

$$\text{Equation 3: } \tau = 0.0070612 K_T(I - I_0)$$

As soon as a motor's torque increases with current, its rotational speed rises with voltage. This angular speed, defined as  $\omega$ , is given in rotations per minute, or *RPM*. The voltage-speed relation closely resembles a straight line. The constant that determines a motor's speed/voltage ratio is called  $K_V$ , and this is usually given in units of *RPM/V* (revolutions per minute per volt). (Kirtley & Beaty, 1998)

Every motor's armature has resistance  $R_a$ . Some of the voltage entering the motor will drop across  $R_a$ , and this voltage loss is referred to as  $V_a$ . If  $V$  is the total voltage applied, the motor's speed equals  $K_V(V - V_a)$ . Knowing the motor's current is  $I - I_0$ , the following equation will be achieved: (Scarpino, 2015)

$$\text{Equation 4: } V_a = (I - I_0) R_a$$

Finally, Scarpino (2015) argues that motors convert input voltage ( $V - V_a$ ) and input current ( $I - I_0$ ) to torque ( $\tau$ ) and speed ( $\omega$ ). This relationship can be expressed by equating the input electrical power to the output mechanical power, which results in the following equation:

$$\text{Equation 5: } (V - V_a)(I - I_0) = \tau\omega$$

## 2.2.5 Stepper Motors

The primary concern in stepper motors is motion control meaning that the motor is to turn with a specific angle and/or speed. To be more specific the main objective of stepper motors is to rotate through a precise angle and then halt. Therefore, the speed and torque of the rotation become the secondary importance. It is necessary to know that one of the significant advantages of stepper motors is that the controller doesn't have to read the stepper's position to define its orientation. (Chen, n.d.)

Stepper motors in practice nowadays can be divided into three categories:

- ❖ Permanent motor (PM)
- ❖ Variable reluctance (VR)
- ❖ Hybrid (HY) - combination of PM and VR steppers' structures

Furthermore, PM and HY stepper motors can be categorized according to their motor windings that affect their control (VR stepper motors are omitted from this categorization in this paper due to their scarcity): (Scarpino, 2015)

- ❖ Bipolar stepper control
- ❖ Unipolar stepper control

### 2.2.6 Permanent Magnet (PM) Steppers

Permanent magnet (PM) steppers are popular in embedded devices such as disk drives and computer printers, due to their small size and reliability. PM steppers are known to have high torque yet poor angular resolution. Figure 13 depicts the ST-PM35 stepper from Mercury Motor. (Scarpino, 2015)



Figure 13 – A permanent magnet (PM) stepper motor. Source: (Scarpino, 2015)

In PM motors permanent magnets are added to the structure of the motor. The rotor no longer has teeth (unlike VR motor), instead the rotor is magnetized with alternating north and south poles that are located in a straight line parallel to the rotor shaft. These magnetized rotor poles provide an increased magnetic flux intensity and because of this the PM motor shows improved torque characteristics when compared with the VR motors. (Ericsson, n.d.)

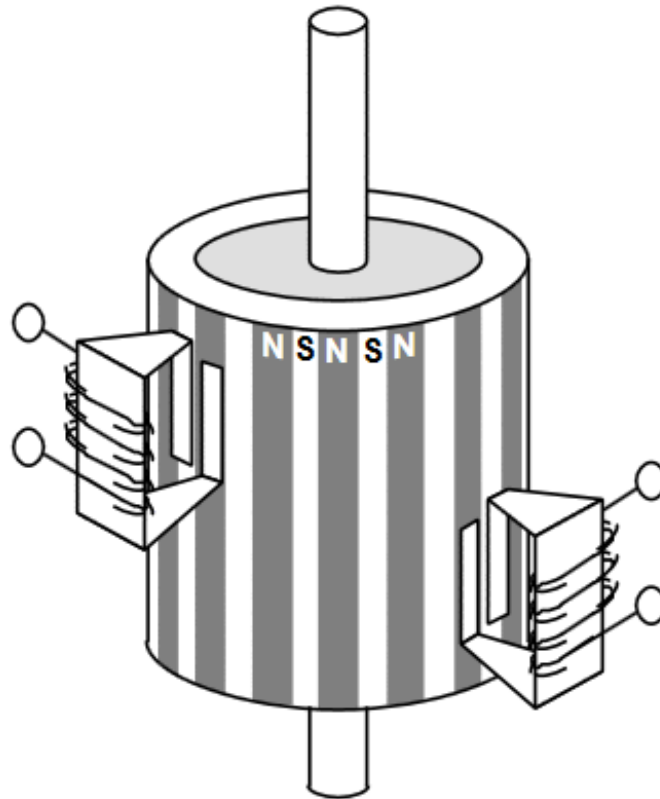


Figure 14 – Principle of a PM or tin-can stepper motor. Source: (Ericsson, n.d.)

### 2.2.7 Variable-reluctance (VR)

This type of motor is comprised of a soft iron multi-toothed rotor and a wound stator. When the stator windings are energized with DC current the poles become magnetized. Rotation happens when the rotor teeth are attracted to the energized stator poles. Figure 15 shows a cross section of a typical VR stepper motor. (Ericsson, n.d.)

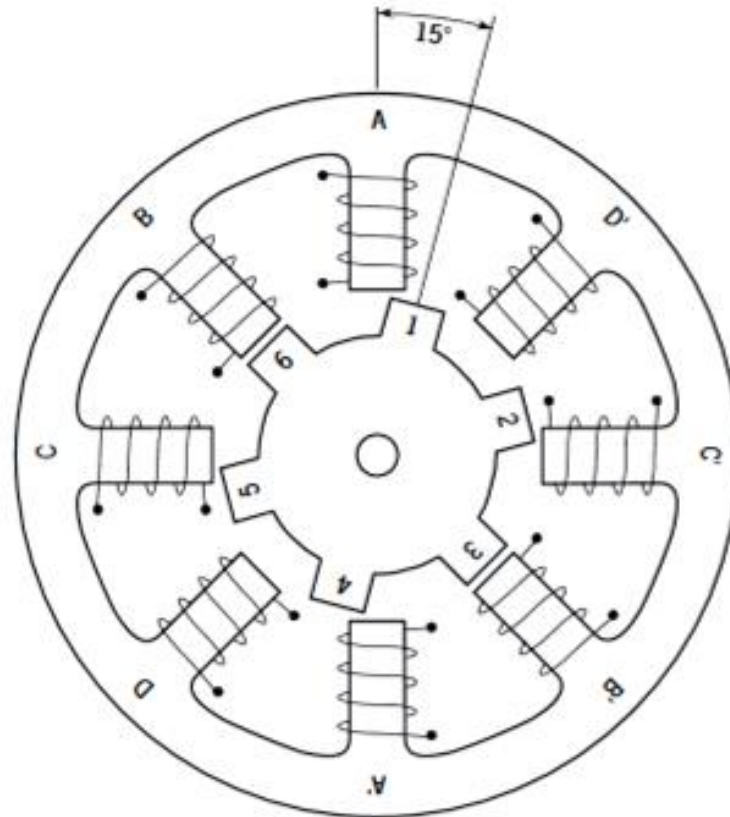


Figure 15 – Cross-section of a variable-reluctance (VR) motor. Source: (Ericsson, n.d.)

In a variable reluctance (VR) stepper, the rotor turns at a particular angle to minimize the reluctance between opposite windings in the stator. Reluctance determines the flow of magnetic flux in a similar way as resistance determining the flow of electric current. The primary advantage of VR steppers is their excellent angular resolution, as their major disadvantage is low torque. (Scarpino, 2015)

### 2.2.8 Hybrid (HY) Steppers

A hybrid (HY) stepper provides the best properties of VR and PM motors due to its structure. Similar to a PM stepper structure, the rotor has magnets that provide torque. Furthermore, Like a VR stepper, the rotor has teeth which results in angular resolution improvement. Figure 16 shows the JK42HW34 hybrid stepper from RioRand. (Kirtley & Beaty, 1998)

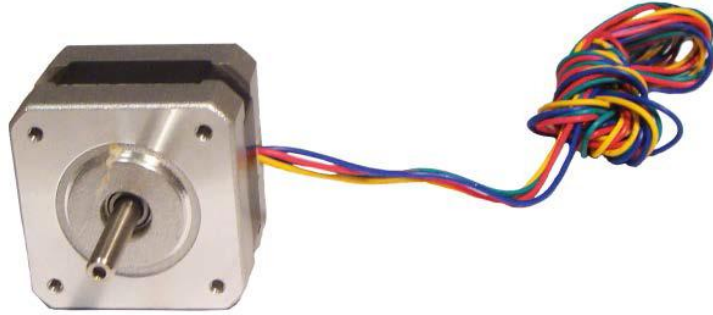


Figure 16 – A hybrid (HY) stepper. Source: (Scarpino, 2015)

### 2.2.9 Bipolar Stepper Control

The terms bipolar and unipolar point out how the wires are connected to the motor's windings. A two-phase bipolar stepper has four wires. Figure 17 shows how the wires are connected inside the stepper. (Hughes, 2006)

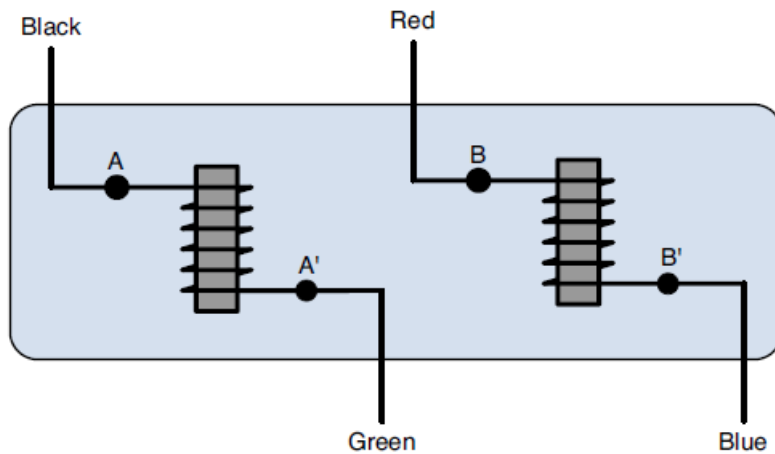


Figure 17 – Connections of a bipolar stepper motor. Source: (Scarpino, 2015)

In figure 17 electromagnets and their corresponding phases are indicated by:  $A/A'$  and  $B/B'$ . According to Scarpino (2015) the electromagnet's poles are resolved by the nature of the current flow. If current flows from the black wire to the green wire,  $A$  will be the north pole and  $A'$  will be the south pole. If current flows from green to black,  $A$  will be the south pole and  $A'$  will be the north pole.

Scarpino (2015) explains further that by providing means of reversing current in the wires it is possible to design a circuit that drives a bipolar stepper. A common method of accomplishing this is by using H bridges. An H bridge is an electronic circuit that includes of four switches that, when opened and closed properly, make it possible to deliver current in the forward and reverse directions.

Figure18 displays how an H-bridge can be connected to control one phase ( $A/A'$ ) of a bipolar motor. This uses four MOSFETs to serve as the switches. The current's direction is controlled by setting voltages on the MOSFET gates which are insulated and their voltage determines the conductivity of the H-bridge. When  $S_0$  and  $S_3$  are set high and  $S_1$  and  $S_2$  are low, current travels from  $A$  to  $A'$ , turning  $A$  to the north pole and  $A'$  to the south pole. When  $S_1$  and  $S_2$  are set high and  $S_0$  and  $S_3$  are low, current travels from  $A'$  to  $A$ , changing  $A'$  to the north pole and  $A$  to the south pole. When  $S_0$  and  $S_2$  are let low, the winding is unenergized. (Scarpino, 2015)

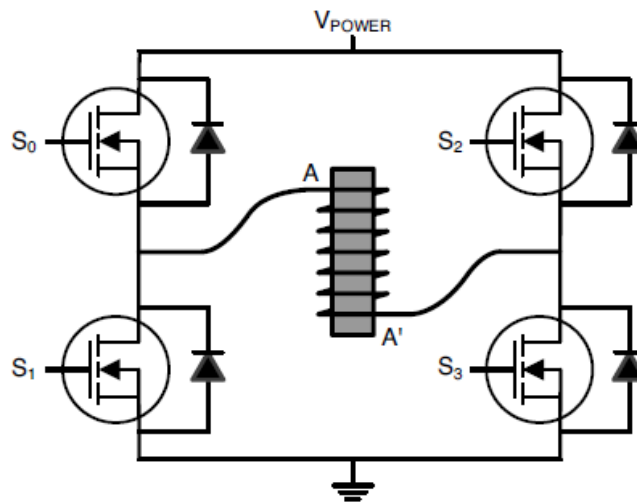


Figure 18 – Controlling one phase of a bipolar stepper with an H bridge. Source: (Scarpino, 2015)

### 2.2.10 Unipolar Stepper Control

Scarpino (2015) asserts that the wiring of a unipolar stepper motor is more complicated than that of a bipolar motor, however, both pursue the same goal: to energize  $A$ ,  $A'$ ,  $B$ , and  $B'$  and to set

their north and south poles accordingly. In figure 19 an example of electromagnet circuits used in unipolar stepper motor structure is displayed.

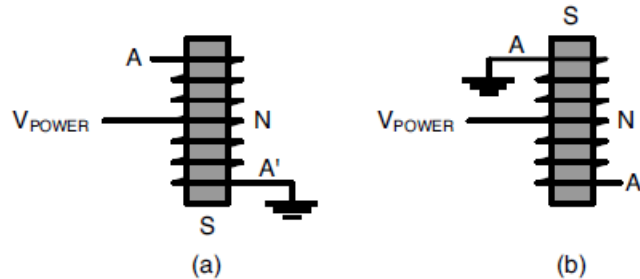


Figure 19 – Electromagnet circuits with a center tap. Source: (Scarpino, 2015)

In both parts a) and b),  $V_{POWER}$  is connected to the center of the electromagnet's winding. This type of connection is called a center tap. In part a), the bottom of the winding is connected to ground. Therefore, current flows from center to the ground, energizing the electromagnet and making the bottom of the winding (labelled as  $A'$ ) the south pole. The north pole is set at the center. (Scarpino, 2015)

While no current flows from the top of the winding to the center, the entire iron core is magnetized by the current in the lower wire, which results in top of the winding behaving as the electromagnet's north pole as well. Therefore, in part a),  $A$  is north and  $A'$  is south. (Hughes, 2006)

In figure 19 part b) displays the reverse situation. The top of the winding is connected to the ground, therefore, current flows from the winding's center to the top which causes the top of the winding ( $A$ ) and the center of the winding become the north pole. Because the entire iron core is magnetized, the bottom of the winding ( $A'$ ) also acts as the north pole. (Scarpino, 2015)

According to Scarpino (2015) in regards to circuit design, controlling a two-phase unipolar stepper requires three steps:

1. Providing  $V_{POWER}$  to the  $A/A'$  and the  $B/B'$  windings.
2. Connecting one wire to ground for each winding in order to set the magnetic poles.

3. Leaving the other wires unconnected.

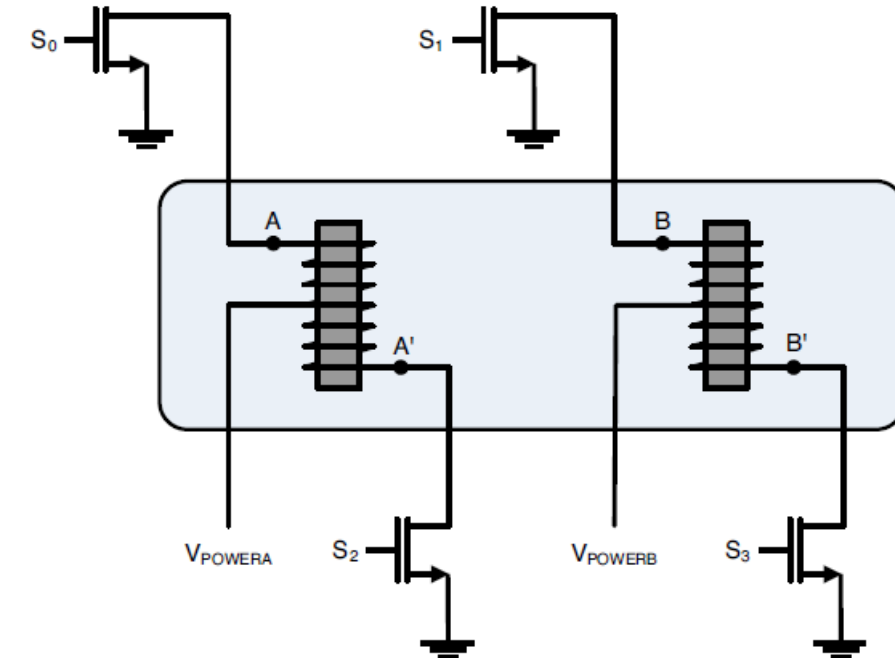


Figure 20 – Connections of a unipolar stepper. Source: (Scarpino, 2015)

Figure 20 displays the six wires entering the unipolar stepper: two wires carry power ( $V_{POWERA}$  and  $V_{POWERB}$ ) and the other four are connected to A, A', B, or B'. Each of the latter four wires is connected to a MOSFET. When the MOSFET's gate voltage overpasses its threshold, the wire is connected to ground; otherwise, the wire is left unconnected. When the MOSFET switches on, the corresponding end of the winding becomes the south pole and the opposite end of the winding becomes the north pole. (Scarpino, 2015)

In unipolar stepper motors that have five wires instead of six, the two supply wires,  $V_{POWERA}$  and  $V_{POWERB}$ , are connected together; and the other four wires remain unchanged. Figure 21 displays a sample diagram for a bipolar stepper and a unipolar stepper motor. (Kirtley & Beaty, 1998)

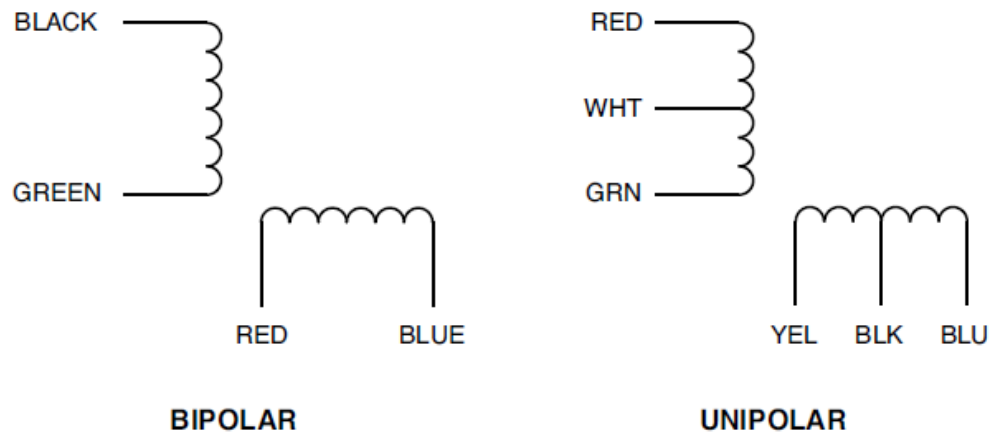


Figure 21 – Sample wiring diagrams in a stepper datasheet. Source: (Kirtley & Beaty, 1998)

### 2.2.11 Servo Motors

Servo Motor or servo is the second type of motor intended for motion control. Whereas stepper motors rotate by an angle and pause, many servos rotate continuously. The main advantage of servos over steppers is that when properly controlled, a servo can perform every task a stepper can and more. In addition to setting the rotation angle, the controller can configure the servo's rotational speed and acceleration. The main disadvantage, however, is that designing a servo controller can be a difficult process. (Drury & Hughes, 2013)

The term servomotor cannot indicate any particular properties about the motor's structure. A servo may be brushed or brushless, AC or DC. The fundamental difference between servomotors and other electric motors is the availability of position feedback. A servo sends a signal to the controller that identifies its rotation angle and/or rotation speed. The controller uses this feedback to resolve what control signals to send. (Scarpino, 2015)



Figure 22 – The FS5106B servomotor from Fitec. Source: (Scarpino, 2015)

Although there is no keen dividing line between servo motors and ordinary motors, the servo type will be intended for use in applications which require rapid acceleration and deceleration. The design of the motor will reflect this by providing intermittent currents (and hence torques) of many times the continuously rate value. (Kirtley & Beaty, 1998)

Many servo motors are utilized in closed-loop position control applications. In figure 23 the angular position of the output shaft is intended to follow the reference voltage, however, if the motor drives a toothed belt, linear outputs can also be acquired. The potentiometer installed on the output shaft provides a feedback voltage proportional to the actual position of the output shaft. The voltage from this potentiometer must be a linear function of angle, and must not vary with temperature; otherwise the accuracy of the system will be affected. (Hughes, 2006)

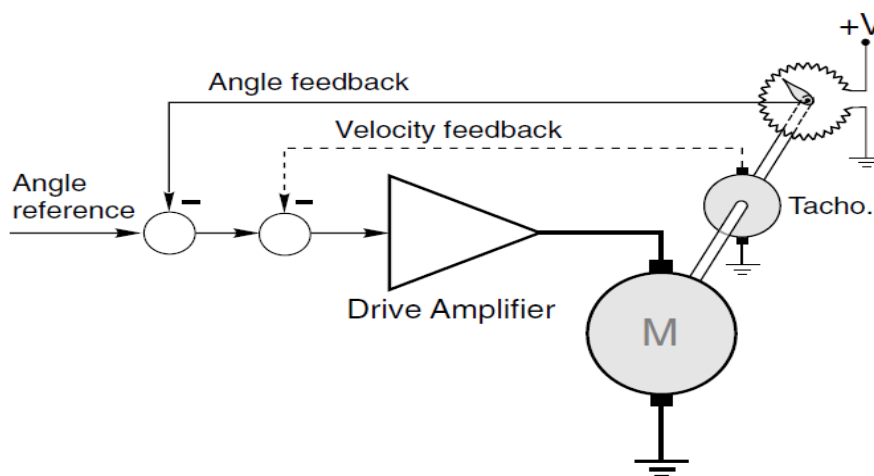


Figure 23 – Closed-loop angular position control using DC motor and angle feedback from a servo-type potentiometer. Source: (Scarpino, 2015)

Hughes (2006) explains that the feedback voltage (standing for the actual angle of the shaft) is subtracted from the reference voltage (standing for the desired position) and the resulting position error signal is amplified and is used to drive the motor in order to rotate the output shaft in the desired direction. Hughes (2006) adds that when the output shaft reaches the target position, the position error becomes zero; therefore, no voltage is applied to the motor, and the output shaft remains at rest. Any attempt to physically move the output shaft from its target position immediately creates a position error and a restoring torque is performed by the motor.

The example mentioned above dealt with an analogue scheme in for the sake of simplicity, but digital position control schemes take priority. Digital implementations have replaced analogue circuitry in many electric drive systems. Digital controllers offer freedom from drift, added flexibility (e.g. programmable ramp-up, ramp-down, maximum and minimum speeds etc.), and simplicity of interfacing and linking to other drives and host computers and controllers, and self-tuning. (Hughes, 2006)

User-friendly diagnostics provides another benefit, providing the local or remote user with current and historical data on the state of all the key drive variables. Many of these advantages are also offered with drives that continue to use analogue control in the power electronic stages. (Drury & Hughes, 2013)

### **3. Main Chapters**

Theoretically it is understood that a solar panel that has the possibility to track the sun has an improved output in comparison to a solar panel that is fixed horizontally. The objective that is perused in this thesis is to design and built a dual-axis tracker that would prove to be economically fruitful as well.

An analysis will be done in order to display that the prototype can also prove economically beneficial.

In order to test this idea a prototype of the solar panel supporting structure and the method for enabling the solar panel to track the sun is designed and constructed.

#### **3.1 Practical Approach**

In the practical part an agile prototype was designed and built with the objective of functioning properly well enough, so that the output voltage of the tracking solar panel could be measured and its optimality over fixed method could be tested.

##### **3.1.1 Solar Panel Supporting Structure**

First of all, for solar panel to be able to have motion, it is required to have a supporting structure that will allow rotating motions both in north-south and east-west directions. Building the structure was realized by using a “Merkur Five Layer Classic Large Kit” from Merkur Company.

For rotating the solar panel in two directions, two motors are required. One motor cannot rotate the solar panel in both directions. The reason is due to the design of the structure.

The body of the structure can be mainly classified into three parts. The first part holds the solar panel. The second part holds the motor that rotates the solar panel in one direction, for example north-south. The first part and the second part are connected to each other by the first axis over which the solar panel rotates in one direction. It is clear that the force of the first motor should be delivered to this axis.

The third part is the base of the structure on which the structure stands on. It also has the second motor attached to it. The second motor rotates the solar panel in the other direction, following the

example above, west-east. The third part and the second part are connected to each other via the second axis. Once again, it is obvious that the second motor force should be fulfilled to the second axis. Therefore, there will be some sort of connection between each axis and their corresponding motor shafts.

It was obvious from the beginning that with this design it is not possible to use only one motor for rotations in both directions. The reasons are that; firstly, a model based on solely one motor requires a certain level of proficiency for sophisticated designs; and secondly, the limitation of accessible materials which had to be used in this thesis for building the structure affects the design of the structure as well.

Another important matter to consider in the design of this structure is the way motors should be attached to the structure. It is not possible to attach the solar panel holder to both axes at the same time, because the movement of the solar panel will become restricted to only the rotation around one axis, and when two axes are attached to the solar panel holder at the same time the solar panel cannot move at all.

That is why the structure consists of three parts and the first motor is attached to the second part and when the second motor in the third part rotates the axis, both the first and second part of the structure rotate around the second axis.

After the construction was built from Merkur kit, it was realized that the first part of the structure is too heavy for the first motor to rotate, and the sum of weight of the first and the second part of the structure is too heavy for the second motor to rotate. Therefore, to solve this problem the first and second parts were printed by a 3D printer in order to decrease the load for both motors. Figure 25 displays the final state of the prototype structure.

Another important detail that is worthy of mentioning here is the way the motors' shafts' forces are transmitted to the axes. Because the solar panel has to maintain its position fixed after finishing tracking, a mechanism should be used in order to prevent the motor's shaft from rotating due to excessive heaviness of the load. This problem is solved by adding worm and wheel gears. Figure 24 displays a pair of worm and wheel gears. The other possibility is to provide constant power to motors; however, it contradicts energy efficiency.

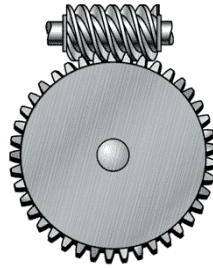


Figure 24 – Worm and wheel gears. Source: (Black, n.d.)

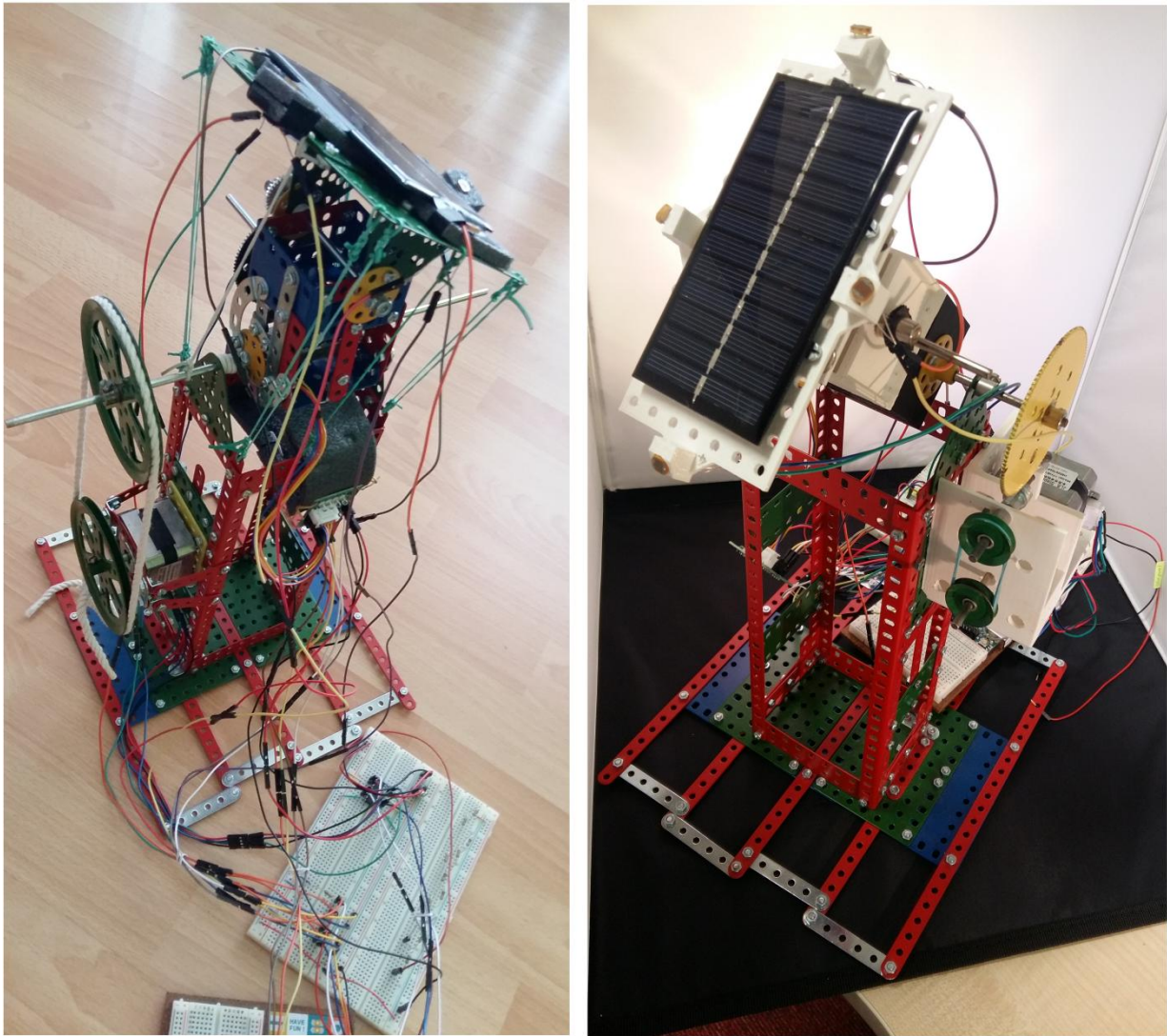


Figure 25 – On the left: Solar panel's supporting structure before final adjustments and improvements. On the right: The final state of the solar panel's supporting structure.

Source: Author

### **3.1.2 Motors**

For choosing the right motors it is important to know that the motors will be able to rotate to a specific angle in a specific direction and then stop, when programmed. For this purpose it is possible to use a servo motor as well as a stepper motor. For the purpose of this prototype stepper motors were chosen over servo motors. That is because stepper motors can be programmed to rotate the shaft in a mode that is called “full step”, in which the motor is able to transmit the most possible force to the shaft that is going to rotate the upper parts of the structure.

For the same reason a unipolar motor was used to rotate the first part of the structure and a bipolar motor was used to rotate the first and second part of the structure. The unipolar motor that is used is smaller and lighter than the bipolar motor. As a result it imposes lesser amount of load for the bipolar motor. Therefore the load which the unipolar motor has to rotate, is also lesser than the load which bipolar motor has to rotate. The bipolar motor can transmit larger force to the motor shaft in full step mode and therefore it is heavier and is attached to the base of the structure.

The unipolar stepper motor is a 28BYJ-48 Stepper Motor with ULN2003 Driver. The bipolar stepper motor is a NEMA-17-SIZE. The datasheets for the motors and the driver can be found in the appendix.

The shafts’ diameter of the motors had to be reduced manually in order to fit the size of the pieces from Merkur kit. That is because it was necessary to secure and transmit the shafts’ force to the axes.

### **3.1.3 Tracking System**

For the solar panel to be capable of tracking the sun, a guiding system must be designed. In order to realize such guiding system, an electronic device sensitive to sunlight should be used to trigger the tracking. Therefore, four photoresistors were used, one pair for north-south direction and one pair for west-east direction, with each of the photoresistors being placed beside one side of the solar panel.

To receive and analyze the output of these photoresistors, and to give commands to the motors to rotate the axes in order to set the solar panel in the proper position (where solar panel will have the most possible output voltage with regard to the position of sun in the sky) based on the result of the analyzed output of the photo resistors, Arduino Uno microcontroller board was used.

Arduino Uno microcontroller board is based on ATmega328, a high-performance microchip according to Geeetech (2014). It consists of 14 digital input/output, 6 analogue inputs, a USB connection, a power jack, oscillator and a reset button. Additionally, it can be programmed with the Arduino software (IDE) provided for all the Arduino series, with the programming language based on C/C++. (Arduino , 2017)

Arduino platform allows receiving data from analogue pins and sending data to an electronic device such as motor through digital pins. Based on these properties an electronic circuit was designed in order to allow the motors to change the solar panel position according to the data that is received by the photoresistors while the output voltage of the solar panel is being saved into a text document with related time and date. Figure 26 and 27 display the breadboard view and schematic view of the designed circuit that were made using Fritzing application, and open-source electronic design automation tool.

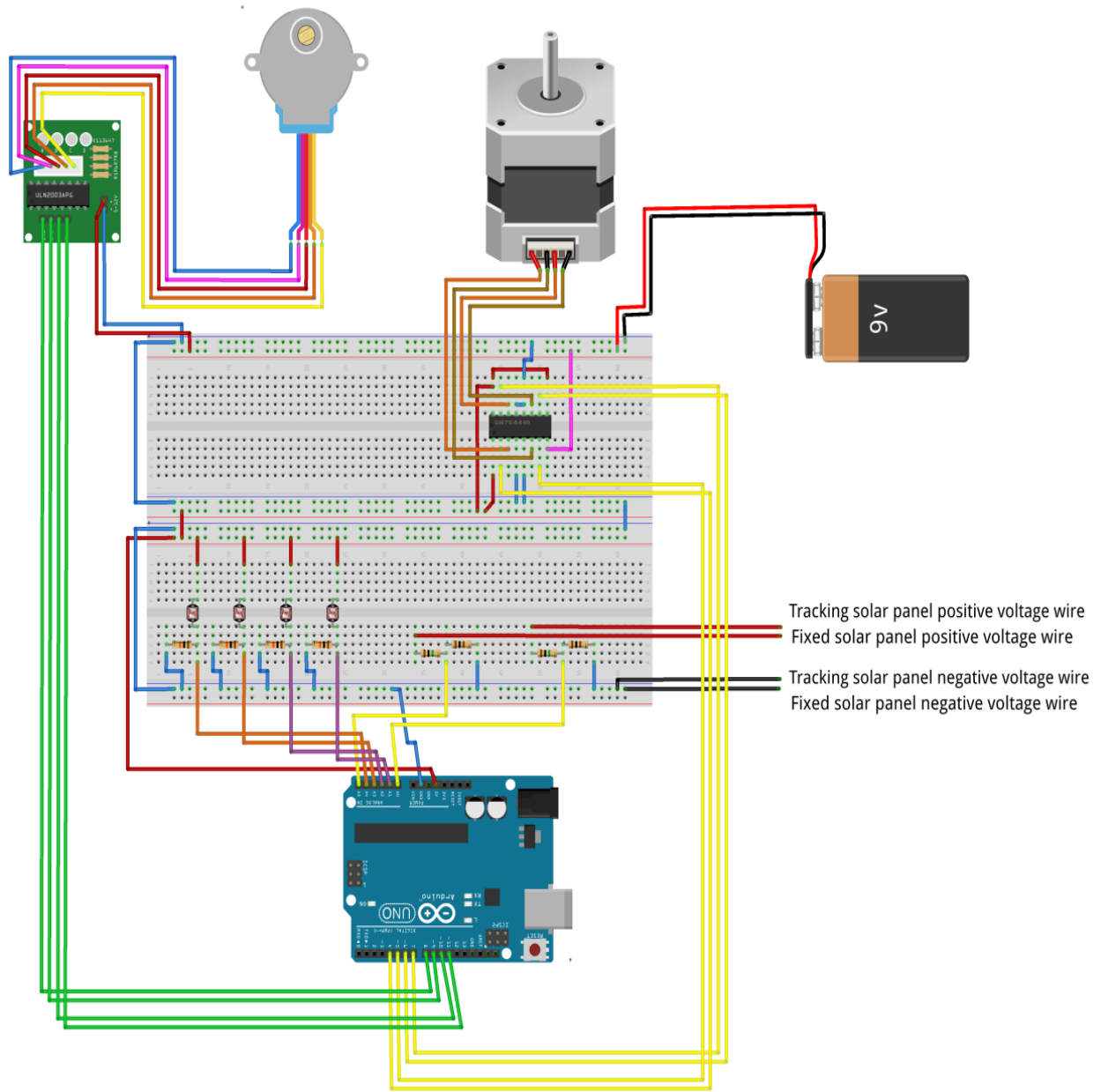
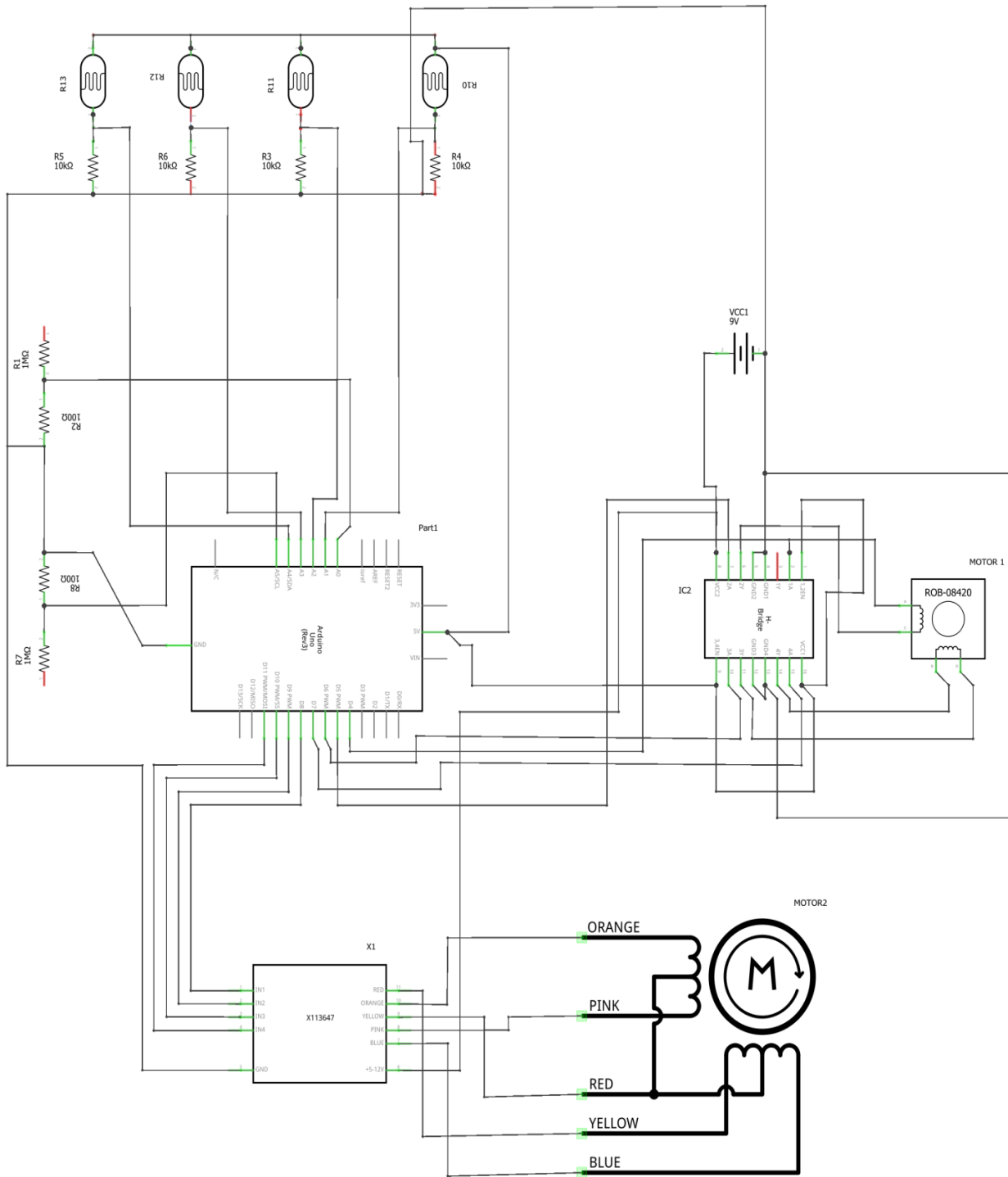


Figure 26 – Breadboard view of the designed prototype circuit. Source: Author.



fritzing

Figure 27 – Schematic view of the designed prototype circuit. Source: Author.

The prototype code that was developed for Arduino Uno can be accessed in appendix – 4. For controlling stepper motors, driver boards can be used because unlike servo motors stepper motors don't have “rest position” or “target position”, and for applications where a stepper motor may need this sense of direction, it would be easier to control them with driver boards.

In the case of this thesis since there was no access to such driver boards for the motors, another method had to be used to limit the rotation of the motor shafts. Because from some point it is not possible for the solar panel holder to move more forward or backward, it will be necessary for the solar panel to rotate only 90° forward or backward from the zenith line. In the method that was used to solve this problem, the rotations of the motor shafts are saved into variables, and boundaries for the value of these variables are declared to prevent the solar panel holder moving more than 90° in both directions.

When the Arduino starts to run the code, the solar panel surface should be parallel to the ground, meaning that the solar panel holder should maintain a 90° position to the horizon and at this position the value of these two variables are set to zero, and the rotations are added or subtracted from changes to this position.

However, if the Arduino is shut down or unplugged the value of these variables will be erased as well from the volatile memory. To avoid this situation and to make sure that the rotations that were counted are not lost the next time that Arduino is turned on; these two variables are saved into EEPROM memory. The data in this memory are kept there when the Arduino is turned off.

Another matter to consider is the output voltage of the solar panels. In order to measure them it is possible to connect the positive wires to Arduino's analogue pins. However, voltages more than the amount, of which that Arduino board can withstand through analogue pins, can harm Arduino. To prevent that from happening, the output voltage of the solar panels is reduced with 1MΩ and 100 KΩ resistors. After Arduino receives the reduced voltage, it is increased to its primary value by particular commands in the code and then is saved to a text file.

Because it is not practical to save all the voltages received from the solar panel into EEPROM memory due to its size, it is required to use another application to transmit and save data from Arduino to a text file. In order to do that Gobetwino free and to-be open source program was used.

Again resistors were used with photoresistors on the board, in order to record the changes in voltage instead of resistance. That is because the analogue to digital convertor in the Arduino read the voltage and converts it into integers.

It can be noticed in the schematics that for controlling the Bipolar motor an H-bridge IC was used.

From a systematic view, the design and construction of the prototype structure was done at the same time when the prototype programming code was designed. However, changes in the design of the structure sometimes required changes in the design of the code during and after the structure was being complete.

## **3.2 Testing**

In order to check the efficiency of the prototype, a test was designed and realized. During the test the output of two identical 6 volts solar panels were recorded in the same environmental condition meaning that they were both tested at the same time and at the same location, with this difference that one of the solar panels was housed by the prototype and the other one was in a fixed horizontal state throughout the testing.

Since the testing required to be done outdoors with no shading casted on the solar panels, and the devices used for testing including a notebook had to use battery power due to lack of access to other power sources, each test had to be done during one hour each time.

In order to include approximately all the possible times during the daylight, the test was done ten times during daytime, starting from 8 am to 6 pm each test being carried out in one separate day. Rainy days and cloudy days (due to rain possibility), were avoided due to the possible damage to the equipments.

The average output voltage of each solar panel for every minute was recorded into a text file. Then after exportation of data in Microsoft Excel, the mean output voltage for each solar panel was calculated.

The final results of output voltage for each test are as following:

Days	1	2	3	4	5	6	7	8	9	10
Hours	8-9	9-10	10-11	11-12	12-13	13-14	14-15	15-16	16-17	17-18
Fixed	1.3	2.7	4	5.3	5.7	5.8	5.4	5.1	4	2.8
Tracker	4.2	4.7	5.3	5.7	5.8	5.9	5.7	5.4	5.1	4.7

Table 1 – Mean output voltage of prototype’solar panel and the fixed solar panel in volts.

Source: Author.

### 3.3 Economical Approach

Another matter to consider is to determine approximately, if it is economical to use this prototype in larger scale. This possibility is tested as an instance depending on the result achieved previously by Gay, et al. (1982) and King, et al. (2002) indicating that in overall, single axis tracker increases annual output by 30% and dual axis tracker by additional 6%, which results in 36% in total. The economical effect of this difference will be examined in the following approximate calculation.

In this calculation it is assumed that solar energy is collected and preserved by two methods at the same time and under the same conditions, with this difference that: in the first method solar panels are horizontally fixed and in the second method the solar panels track the sun by dual-axis using similar technique as the prototype in this paper. It is assumed that this computation is done for Hradec Králové region in Czech Republic.

Firstly, it is assumed that the solar panels used in the model are 300W Prepaid off Grid Outdoor Stand Alone Solar Panels that are purchased from Zhejiang Yuanzhong Solar Co., Ltd.. The considered properties of the solar panels are as following:

Price:	approx. 145\$/Piece	Application:	Industrial
Minimum order:	200 Pieces	Wight per piece:	18.6 Kg
Waranty:	25 Years	Size of panel:	1650 × 992 × 35 mm
Peak power watts- PMAX(WP)	300 W	Operational Temperature:	−40 ~ +85°C

Table 2 – Selected properties of 300W Prepaid off Grid Outdoor Stand Alone Solar Panel.

Source: (Zhejiang Yuanzhong Solar Co., Ltd., 2017).

According to TZB-info.cz (2017), average yearly sunshine collected in Hradec Králové is 1521 hour per year. Knowing that it is possible to calculate the average yearly watts collected by one solar panel, that is the Peak power watts- PMAX(WP) for each solar panel multiplied by average yearly sunshine collected. (Zientara, 2017)

For the dual-axis tracker method it is required to use two stepper motors that could rotate and withstand the weight of each solar panel. For this purpose it is assumed that for each solar panel two 57BYGH gear reducer stepper motor engine Nema 23 from Maintex<sup>®</sup> and one High-precision 2H845 Hybrid 2-phase stepper motor driver for high torque 1.4-5.6A nema 23 stepper motor from Casun<sup>®</sup> are purchased.

The price of each stepper motor is approximately 13 dollars and minimum order is 100 pieces. (Maintex<sup>®</sup>, 2017) The price of each driver is approximately 8 dollars. (Casun<sup>®</sup>, 2017)

Assuming in each method 200 solar panels are purchased. In dual-axis tracker method 400 stepper motors and 400 drivers are purchased additionally. The rest of the costs such as maintenance and installation costs are considered approximately equal in both methods, therefore, they are omitted from the calculation.

Therefore, in ten years, the total solar energy received and total costs for each method will be as following:

Dual-axis Tracking Method	Fixed Panel Method
$300 \times 200 \times 1521 \times 10 =$ <b>912,600,000 kilowatt hour</b>	$300 \times 200 \times 1521 \times 10 \times 64/100 =$ <b>584,064,000 kilowatt hour</b>
$(145 \times 200) + (13 \times 400) + (8 \times 400) =$ <b>39,400 \$ = approx. 895,744 czk</b>	$145 \times 200 =$ <b>31,000 \$ = approx. 704,772 czk</b>

Table 3 – Total solar energy recieved and total costs for dual-axis tracking and fixed solar panel methods. Source: Author.

Knowing that electricity in Czech Republic costs 10.47 cents or approximately 2.38 czk per kilowatt hour according to WorldAtlas.com (2017); in dual-axis tracking method  $912,600,000 \times 2.38 = 2,171,988,000$  czk was saved in electricity consumption and in fixed panel method  $548,064,000 \times 2.38 = 1,304,392,320$  czk was saved. Therefore, subtracting the total costs; 2,171,092,256 czk is saved in total in electricity consumption in dual-axis tracking method, and 1,303,687,548 czk in fixed panel method.

Another matter that was not mentioned during the calculations was the current the motors use to rotate the solar panels. That is because these motors make limited number of rotations per day in sunny days in normal situation and also, calculating the amount of current each of these motors approximately use per year is out of the scope of this paper. However, one possible way to compensate for the current used by the motors could be by adding more solar panels that contribute to the energy used by the motors.

Comparing the results, it is concluded that dual-axis tracking method proves to be more economical method of producing energy compared to the fixed panel method. In this calculation it was observed that it is possible to reduced electricity costs by using dual-axis solar panel trackers almost two times more than when using fixed solar panels in large scale.

## 4. Results

Despite of the problems encountered while designing and building the prototype, the prototype could succeed to function successfully. Due to the limits in resources, minor flaws in the structure remained unsolved. For instance, the solar panel housing could not reach the exact vertical position, yet it could reach an enough close position to the vertical position, in order to be suitable and efficient for testing. The code for the Arduino Uno can be further improved, so that the prototype can operate more swiftly.

Therefore, even though the prototype could not operate ideally, it could operate well enough to be tested. Testing results of the prototype indicate that the prototype increased the output voltage by 13% in comparison with a fixed solar panel.

The same calculation that was done in the “Economical Approach” in order to prove the profitability of prototype based on the research result from Gay, et al. (1982) and King, et al. (2002) , was done again; this time, based on the result obtained from the testing of the prototype that indicates the increase in the output voltage by 13%. The outcome is as following:

Dual-axis Tracking Method	Fixed Panel Method
$300 \times 200 \times 1521 \times 10 =$ <b>912,600,000 kilowatt hour</b>	$300 \times 200 \times 1521 \times 10 \times \frac{87}{100} =$ <b>793,962,000 kilowatt hour</b>

Table 4 – Total solar energy recieved for dual-axis tracking and fixed panel methods based on the testing result of the prototype. Source: Author.

Thus, the prototype proved successfully economically more profitable as well in large scale, compare to the horizontally fixed solar panel method of collecting solar energy even based on the results from the prototype test.

## 5. Conclusions and Recommendations

Although storing energy seems to be more costly with dual axis solar tracker compare to a fixed solar panel in short term, it is proven to be more beneficial economically in long term according to the analysis and experiments in this paper. This difference appears greater especially when the solar panels are used in a large scale.

It is important to use enough sturdy, yet as light materials as possible for the designing of the part of the structure to which solar panel and one of the motors are attached. The gears that transmit power from motors to the axis should have complete and sturdy engagement in order for motors to be able to rotate the solar panel when needed efficiently.

It may prove beneficial to use Bluetooth technology for the sake of controlling and monitoring the solar tracker performance and output. For instance, turning on and off the tracking system; or receiving an instant message in case of system failure.

Another alternative suggested is Sigfox technology, an IoT wireless network system. Through this technology it is possible to connect low energy objects and therefore the tracker can become part of an IoT ecosystem.

Finally, the tracking system can be equipped by LoRa wireless technology for instance in domestic domain of IoT.

## Bibliography

Adafruit, 2017. *Stepper motor - NEMA-17 size - 200 steps/rev, 12V 350mA*. [Online]  
Available at: <https://www.adafruit.com/product/324>  
[Accessed 26 March 2017].

Arduino , 2017. *Language Reference*. [Online]  
Available at: <https://www.arduino.cc/en/Reference/HomePage>  
[Accessed 23 May 2017].

Arduino, 2017. *Arduino Homepage*. [Online]  
Available at: <https://www.arduino.cc/>  
[Accessed 28 March 2017].

Black, A., n.d. *The Ins and Outs of Worm Gears*. [Online]  
Available at: <http://machinerylubrication.com/Read/1080/worm-gears>  
[Accessed 25 March 2017].

Boysen, E. & Kybett, H., 2012. *Complete Electronics Self-Teaching Guide with Projects*..  
s.l.:Wiley.

Brynjolfsson, E. & McAfee, A., 2016. *The Second Machine Age: Work, Progress, and Prosperity in a Time of Brilliant*. s.l.:W. W. Norton & Company..

Casun ® , 2017. *High-Precision 2H845 Hybrid 2-Phase Stepper Motor Driver, High Torque 1.4-5.6A Nema 23 Stepper Motor Driver*. [Online]  
Available at: [https://www.alibaba.com/product-detail/High-precision-2H845-hybrid-2-phase\\_60039008918.html](https://www.alibaba.com/product-detail/High-precision-2H845-hybrid-2-phase_60039008918.html)  
[Accessed 3 July 2017].

Chen, B. M., n.d. *Ben M. Chen's Teaching Page*. [Online]  
Available at: <http://uav.ece.nus.edu.sg/~bmchen/>  
[Accessed 6 December 2016].

Drury, B. & Hughes, A., 2013. *Electric Motors and Drives: Fundamentals, Types and Applications*. 4th ed. s.l.:Newnes.

Dunlop, J. I. p. w. N., 2009. *Photovoltaic Systems Engineering*. s.l.:Amer Technical.

Ericsson, n.d. *Jonathan W. Valvano*. [Online]  
Available at: <http://users.ece.utexas.edu/~valvano/Datasheets/StepperBasic.pdf>  
[Accessed 22 February 2017].

Ertekin, C., Evrendilek, F. & Kulcu, R., 2008. Modeling Spatio-Temporal Dynamics of Optimum Tilt Angles for Solar Collectors in Turkey. *Sensors (Basel, Switzerland)*, May, Volume 8(5), pp. 2913-2931.

Fitzge, S. & Shiloh, M., 2012. *Arduino Projects Book*. Torino: Arduino LLC.

Fritzing, 2017. *Fritzing*. [Online]  
Available at: <http://fritzing.org/home/>  
[Accessed 30 March 2017].

Gay, F. C., Yerkes, J. W. & Wilson, J. H., 1982. Performance advantages of two-axis tracking for large flat-plate photovoltaic energy systems. *Photovoltaic Specialists Conference. Institute of Electrical and Electronics Engineers.*, September, Volume 16, pp. 1368-1371.

Geeetech, 2014. *Arduino Uno*. [Online]  
Available at: [http://www.geeetech.com/wiki/index.php/Arduino\\_Uno](http://www.geeetech.com/wiki/index.php/Arduino_Uno)  
[Accessed 17 May 2017].

Hughes, A., 2006. *Electric Motors and Drives: Fundamentals, Types and Applications*. 3rd ed. s.l.:Elsevier Ltd..

Kernighan, B. W. & Ritchie, D. M., 1988. *The C Programming Language*. s.l.:Prentice Hall PTR.

Kiatronics, 2017. *28BYJ-48 Stepper Motor 5VDC - Code: 70289*. [Online]  
Available at: <http://www.kiatronics.com/motors/28byj-48-stepper-motor-5vdc-code-70289.html>  
[Accessed 26 March 2017].

kiatronics, 2017. *ULN2003 Stepper Motor Driver PCB - Code: 70285*. [Online]  
Available at: <http://www.kiatronics.com/motors/uln2003-stepper-motor-driver-pcb.html>  
[Accessed 26 March 2017].

King, D. L., Boyson, W. E. & Kratochvil, J. A., 2002. Analysis of factors influencing the annual energy production of photovoltaic systems. *Photovoltaic Specialists Conference. Conference Record of the Twenty-Ninth IEEE*..

Kirtley, J. & Beaty, W. H., 1998. *Electric Motor Handbook*. 1st ed. s.l.:McGraw-Hill Education.

Lv, Y. et al., 2016. An Optimized Model for Solar Thermal Collectors Based on Concept of Effective Heat Collection. *Energy Procedia*, June, Volume 88, pp. 470-475.

Maintex ® , 2017. *57BYGH Gear Reducer Stepper Motor Engine Nema 23 Motor Parts*. [Online]  
Available at: <https://www.alibaba.com/product-detail/57BYGH-Gear-Reducer-Stepper-Motor->

[Engine\\_60634305525.html?s=p](#)

[Accessed 3 July 2017].

Marion, W. & Wilcox, S., 1994. *Solar Radiation Data Manual for Flat-Plate and Concentrating Collectors*. Colorado: National Renewable Energy Laboratory.

Merkur, 2017. *Merkur*. [Online]

Available at: <http://www.merkurtoys.cz/>

[Accessed 26 March 2017].

Messenger, R. & Ventre, J., 2004. *Photovoltaic systems engineering*. 2nd ed. s.l.:CRC Press LLC.

MikMo, 2011. *Gobetwino*. [Online]

Available at: <http://mikmo.dk/gobetwino.html>

[Accessed 2 February 2017].

Monk, S., 2016. *Raspberry Pi Cookbook: Software and Hardware Problems and Solutions*. s.l.:O'Reilly Media.

Purdum, J., 2015. *Beginning C for Arduino*. 1st ed. s.l.:Apress.

Scarpino, M., 2015. *Motors for Makers: A Guide to Steppers, Servos, and Other Electrical Machines*. s.l.:Que Publishing.

Solar Energy Research Institute, 1982. *Basic Photovoltaic Principles and Methods*. Washington, DC: U.S. Government Printing Office.

Stanciu, C. & Stanciu, D., 2014. Optimum tilt angle for flat plate collectors all over the World – A declination dependence formula and comparisons of three solar radiation models. *Energy Conversion and Management*, Volume 81, pp. 133-143.

Sukhatme, S. P. & Sukhatme, K., 1996. *Principles of Thermal Collection and Storage*. s.l.:Tata McGraw-Hill Education.

Townsend, K., Cufí, C., Davidson, A. & Davidson, R., 2014. *Getting Started with Bluetooth Low Energy: Tools and Techniques for Low-Power Networking*. s.l.:O'Reilly Media.

TZB-info.cz, 2017. *Průměrné měsíční doby slunečního svitu ve vybraných lokalitách ČR*.

[Online]

Available at: <http://www.tzb-info.cz/tabulky-a-vypocty/99-prumerne-mesicni-doby-slunecniho-svitu-ve-vybranych-lokalitach-cr>

[Accessed 3 July 2017].

WorldAtlas.com, 2017. *Cost Of Electricity By Country*. [Online]  
Available at: <http://www.worldatlas.com/articles/electricity-rates-around-the-world.html>  
[Accessed 5 July 2017].

Zhejiang Yuanzhong Solar Co., Ltd., 2017. *300W Prepaid off Grid Outdoor Stand Alone Solar Energy Solar System*. [Online]  
Available at: <http://yzrichsolar.en.made-in-china.com/product/XCLmvRKkXThp/China-300W-Prepaid-off-Grid-Outdoor-Stand-Alone-Solar-Energy-Solar-System.html>  
[Accessed 3 July 2017].

Zientara, B., 2017. *How much electricity does a solar panel produce?*. [Online]  
Available at: <https://solarpowerrocks.com/solar-basics/how-much-electricity-does-a-solar-panel-produce/>  
[Accessed 3 July 2017].

# Appendix

Appendix 1 – Unipolar motor’s datasheet. Source: (Kiatronics, 2017)

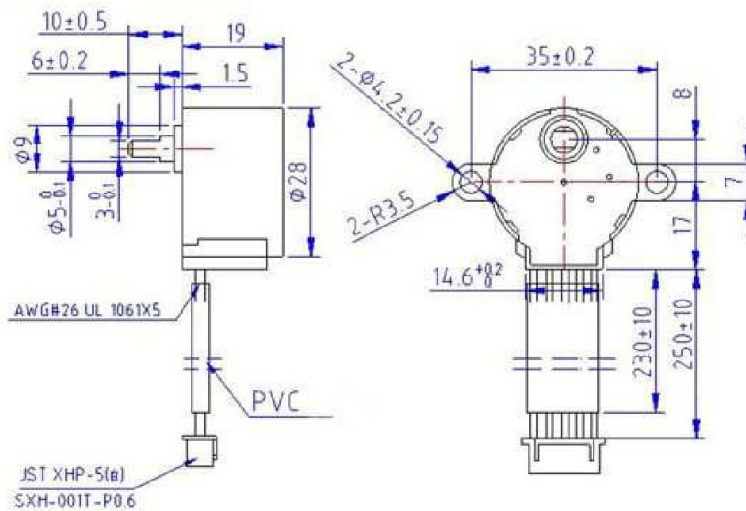
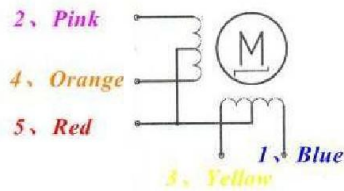
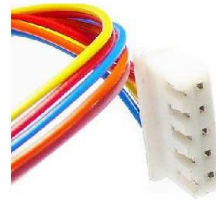


## 28BYJ-48 – 5V Stepper Motor

The 28BYJ-48 is a small stepper motor suitable for a large range of applications.

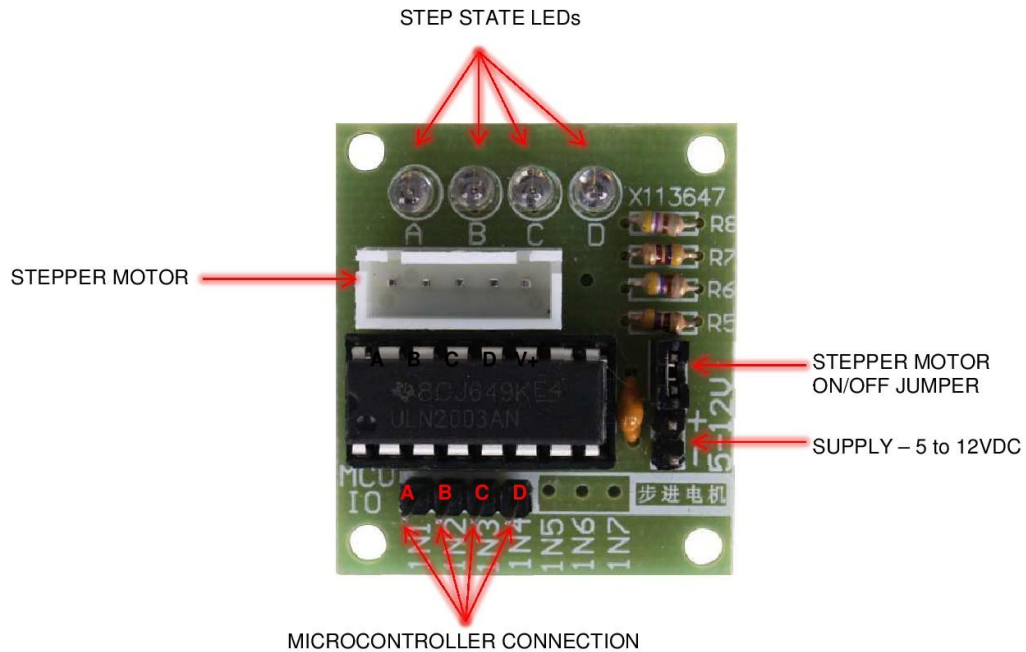


Rated voltage :	5VDC
Number of Phase	4
Speed Variation Ratio	1/64
Stride Angle	5.625°/64
Frequency	100Hz
DC resistance	50Ω±7%(25°C)
Idle In-traction Frequency	> 600Hz
Idle Out-traction Frequency	> 1000Hz
In-traction Torque	>34.3mN.m(120Hz)
Self-positioning Torque	>34.3mN.m
Friction torque	600-1200 gf.cm
Pull in torque	300 gf.cm
Insulated resistance	>10MΩ(500V)
Insulated electricity power	600VAC/1mA/1s
Insulation grade	A
Rise in Temperature	<40K(120Hz)
Noise	<35dB(120Hz, No load, 10cm)
Model	28BYJ-48 – 5V



### 4 Phase ULN2003 Stepper Motor Driver PCB

The ULN2003 stepper motor driver PCB provides a direct drive interface between your microcontroller and stepper motor. The PCB provides 4 inputs for connection to your microcontroller, power supply connection for the stepper motor voltage, and ON/OFF jumper, a direct connect stepper motor header and 4 LEDs to indicate stepping state.



#### Stepper Motor Connection

Connect stepper motor to this header. If you use one of our stepper motors they will just plug directly into the header. If you have another brand without the correct header plug, you could solder the wires directly to the back of the PCB.

#### Step State LEDs

Indicate which channel is active.

#### ON/OFF Jumper

Isolates power to the stepper Motor

#### Supply

Power to drive stepper motor. Make sure it matches the rating of the stepper motor you are using.

#### Microcontroller Connection

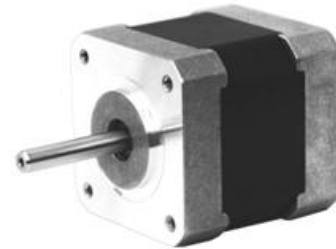
Connect 4 outputs from your microcontroller to the four inputs.

Supply Volts: 5-12VDC

Maximum Current per output : 500mA

### 1.8° 42MM High Torque Hybrid Stepping Motor

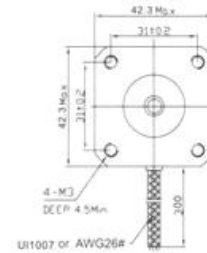
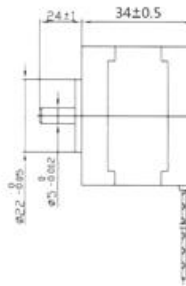
Item	Specifications
Step Angle	1.8°
Step Angle Accuracy	±5% ( full step, no load )
Resistance Accuracy	±10%
Inductance Accuracy	±20%
Temperatru Rise	80°CMax. ( rated current,2 phase on )
Ambient Temperatuar	-20°C~+50°C
Insulation Resistance	100M?Min.,500VDC
Dielectric Strength	500VAC/ for one minute
Shaft Radial Play	0.02Max. ( 450 g-load )
Shaft Axial Play	0.08Max. ( 450 g-load )
Max. radial force	28N ( 20mm foom the flange )
Max.axial force	10N



### ● 42MM Hybrid Stepping Motor Specifiers

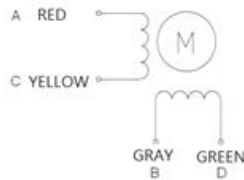
Model No	Rated Voltage	Current /Phase	Resistance /Phase	Inductance /Phase	Holding Torque	# of Leads	Rotor Inertia	Weight	Detent Torque	Length
XY42STH34-0354A	V	A	Ω	mH	Kg-cm		g-cm <sup>2</sup>	kg	g-cm	mm
	12	0.35	34	33	1.6	4	35	0.22	120	34

### ● Dimension

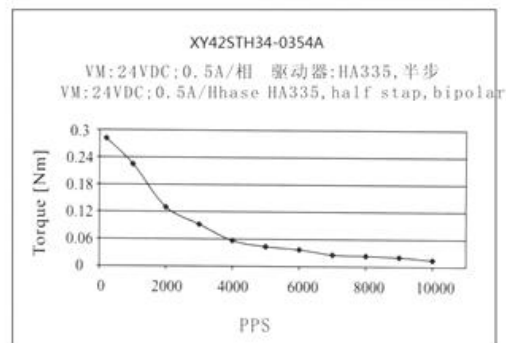


### ● Wiring Diagram

4 LEADS



### ● Pull out Torque Curve



#### Appendix 4 – Prototype code developed for Arduino Uno. Source: Author.

```
#include <Stepper.h>
#include <avr/interrupt.h>
#include <avr/eeprom.h>

#define uniMotorPin1 8
#define uniMotorPin2 9
#define uniMotorPin3 10
#define uniMotorPin4 11

#define biMotorPin1 4
#define biMotorPin2 5
#define biMotorPin3 6
#define biMotorPin4 7

#define stepFLimitUniPM 576
#define stepBLimitUniPM -576
#define stepFLimitBiPM 882
#define stepBLimitBiPM -882

#define phr1UniPMPin A1
#define phr2UniPMPin A2
#define phr1BiPMPin A3
#define phr2BiPMPin A4

#define solarPanelPin A0
float solarPanelOutput = 0.0;
float prevSolarPanelOutput = 0.0;

int sumPhr1BiPM = 0;
int sumPhr2BiPM = 0;
int sumPhr1UniPM = 0;
int sumPhr2UniPM = 0;

int phr1UniPMValue = 0;
int phr2UniPMValue = 0;
int phr1BiPMValue = 0;
int phr2BiPMValue = 0;

int prevPhr1UniPMValue = 0;
int prevPhr2UniPMValue = 0;
int prevPhr1BiPMValue = 0;
int prevPhr2BiPMValue = 0;

#define numSamples 6
int sum = 0; // sum of samples taken
unsigned char sampleCount = 0;
int count = 0;

int shortDelay = 10;
int Steps = 0;
```

```

int stepCountUniPM = 0;
int stepCountBiPM = 0;

int addressUniPM = 0;
int addressBiPM = 1;
int readValue = 0;

int i = 0;

boolean ClockwiseMotion = true;

void setup() {

  pinMode(uniMotorPin1, OUTPUT);
  pinMode(uniMotorPin2, OUTPUT);
  pinMode(uniMotorPin3, OUTPUT);
  pinMode(uniMotorPin4, OUTPUT);

  pinMode(biMotorPin1, OUTPUT);
  pinMode(biMotorPin2, OUTPUT);
  pinMode(biMotorPin3, OUTPUT);
  pinMode(biMotorPin4, OUTPUT);

  pinMode(solarPanelPin, INPUT);

  while (!Serial);
  Serial.begin(9600);
  Serial.print("#S|LOGDATA|[]#");
  Serial.print("#S|T|[]#");
  Serial.print("#S|D|[]#");

  while (!eeprom_is_ready()); // Waiting for EEPROM to be ready
  cli();
  eeprom_write_word((uint16_t*)addressUniPM, stepCountUniPM); //
  initialize step value into EEPROM
  sei();
  eeprom_write_word((uint16_t*)addressBiPM, stepCountBiPM);
  sei();
}

void loop() {

  while (sampleCount < numSamples) {

    sumPhr1UniPM += analogRead(phr1UniPMPin);
    sumPhr2UniPM += analogRead(phr2UniPMPin);
    sumPhr1BiPM += analogRead(phr1BiPMPin);
    sumPhr2BiPM += analogRead(phr2BiPMPin);
    sampleCount++;
    delay(shortDelay);
  }
}

```

```

phr1UniPMValue = sumPhr1UniPM/10;
phr2UniPMValue = sumPhr2UniPM/10;
phr1BiPMValue = sumPhr1BiPM/10;
phr2BiPMValue = sumPhr2BiPM/10;

Serial.println(" ");
Serial.print("resistor 1 for UniPolarMotor: ");
Serial.print(phr1UniPMValue);
Serial.print(" /resistor2 for UniPolarMotor: ");
Serial.println(phr2UniPMValue);

Serial.print("resistor 1 for BiPolarMotorr: ");
Serial.print(phr1BiPMValue);
Serial.print(" /resistor2 for BiPolarMotorr: ");
Serial.println(phr2BiPMValue);
delay(shortDelay);

while (sampleCount < numSamples) {
    sum += analogRead(solarPanelPin);
    sampleCount++;
    delay(10000);
}

solarPanelOutput = ((float)sum / (float)numSamples * 5) / 1024;
Serial.print(solarPanelOutput * 11);
Serial.println (" V");
sampleCount = 0;
sum = 0;

Serial.print("#S|LOGDATA|[");
Serial.print(" ");
Serial.print(float(solarPanelOutput * 11) , 2);
Serial.print(" ; ");
Serial.print(float(solarPanelOutput * 11) , 2);
Serial.println("]#");

if ( abs(solarPanelOutput - prevSolarPanelOutput) > 3 ) sweep();

if (phr2UniPMValue < phr1UniPMValue) unipolarMoveForward();
else if (phr2UniPMValue > phr1UniPMValue) unipolarMoveBackward();
else uniPStepper(0);

if (phr2BiPMValue < phr1BiPMValue) bipolarMoveForward();
else if (phr2BiPMValue > phr1BiPMValue) bipolarMoveBackward();
else biPStepper(0);

prevSolarPanelOutput = solarPanelOutput;

while (!eeprom_is_ready());
cli();
if(eeprom_read_word((uint16_t*)addressUniPM) != stepCountUniPM) {
    eeprom_write_word((uint16_t*)addressUniPM, stepCountUniPM);
}
sei();

```

```

while (!eeprom_is_ready());
cli();
if(eeprom_read_word((uint16_t*)addressBiPM) != stepCountBiPM) {
    eeprom_write_word((uint16_t*)addressBiPM, stepCountBiPM);
}
sei();
}

void setDirection(){
    if (ClockwiseMotion) {
        Steps++;
    } else {
        Steps--;
    }
    if(Steps>3){
        Steps=0;
    } else if(Steps<0){
        Steps=3;
    }
}

void uniPStepper(int num){
    for (int i=0; i<num; i++){
        switch(Steps){
            case 1:
                digitalWrite(uniMotorPin1, HIGH);
                digitalWrite(uniMotorPin2, LOW);
                digitalWrite(uniMotorPin3, LOW);
                digitalWrite(uniMotorPin4, HIGH);
                break;
            case 2:
                digitalWrite(uniMotorPin1, HIGH);
                digitalWrite(uniMotorPin2, HIGH);
                digitalWrite(uniMotorPin3, LOW);
                digitalWrite(uniMotorPin4, LOW);
                break;
            case 3:
                digitalWrite(uniMotorPin1, LOW);
                digitalWrite(uniMotorPin2, HIGH);
                digitalWrite(uniMotorPin3, HIGH);
                digitalWrite(uniMotorPin4, LOW);
                break;
            case 4:
                digitalWrite(uniMotorPin1, LOW);
                digitalWrite(uniMotorPin2, LOW);
                digitalWrite(uniMotorPin3, HIGH);
                digitalWrite(uniMotorPin4, HIGH);
                break;
            default:
                digitalWrite(uniMotorPin1, LOW);
                digitalWrite(uniMotorPin2, LOW);
                digitalWrite(uniMotorPin3, LOW);
                digitalWrite(uniMotorPin4, LOW);
        }
    }
}

```

```

        break;
    }
    setDirection();
}
}

void biPStepper(int num){
    for (int i=0; i<num; i++){
        switch(Steps){
            case 1:
                digitalWrite(biMotorPin1, HIGH);
                digitalWrite(biMotorPin2, LOW);
                digitalWrite(biMotorPin3, HIGH);
                digitalWrite(biMotorPin4, LOW);
                break;
            case 2:
                digitalWrite(biMotorPin1, LOW);
                digitalWrite(biMotorPin2, HIGH);
                digitalWrite(biMotorPin3, HIGH);
                digitalWrite(biMotorPin4, LOW);
                break;
            case 3:
                digitalWrite(biMotorPin1, LOW);
                digitalWrite(biMotorPin2, HIGH);
                digitalWrite(biMotorPin3, LOW);
                digitalWrite(biMotorPin4, HIGH);
                break;
            case 4:
                digitalWrite(biMotorPin1, HIGH);
                digitalWrite(biMotorPin2, LOW);
                digitalWrite(biMotorPin3, LOW);
                digitalWrite(biMotorPin4, HIGH);
                break;
            default:
                digitalWrite(biMotorPin1, LOW);
                digitalWrite(biMotorPin2, LOW);
                digitalWrite(biMotorPin3, LOW);
                digitalWrite(biMotorPin4, LOW);
                break;
        }
        setDirection();
    }
}

void unipolarMoveBackward() {
    while (phr2UniPMValue > phr1UniPMValue & stepCountUniPM <
stepFLimitUniPM){
        uniPStepper(32);
        stepCountUniPM = stepCountUniPM + 32;
        delay(shortDelay);
    }

    while (sampleCount < numSamples) {

```

```

        sumPhr1UniPM += analogRead(phr1UniPMPin);
        sumPhr2UniPM += analogRead(phr2UniPMPin);
        sampleCount++;
        delay(shortDelay);
    }
    phr1UniPMValue = sumPhr1UniPM/10;
    phr2UniPMValue = sumPhr2UniPM/10;
    delay(shortDelay);
}

void unipolarMoveForward() {
    while (phr2UniPMValue < phr1UniPMValue & stepCountUniPM >
stepBLimitUniPM) {
        uniPStepper(-32);
        stepCountUniPM = stepCountUniPM - 32;
        delay(shortDelay);
    }
    while (sampleCount < numSamples) {

        sumPhr1UniPM += analogRead(phr1UniPMPin);
        sumPhr2UniPM += analogRead(phr2UniPMPin);
        sampleCount++;
        delay(shortDelay);
    }
    phr1UniPMValue = sumPhr1UniPM/10;
    phr2UniPMValue = sumPhr2UniPM/10;
    delay(shortDelay);
}

void bipolarMoveForward() {
    while (phr2BiPMValue > phr1BiPMValue & stepCountBiPM <
stepFLimitBiPM) {
        biPStepper(49);
        stepCountBiPM = stepCountBiPM + 49;
        delay(shortDelay);
    }

    while (sampleCount < numSamples) {
        sumPhr1BiPM += analogRead(phr1BiPMPin);
        sumPhr2BiPM += analogRead(phr2BiPMPin);
        sampleCount++;
        delay(shortDelay);
    }

    phr1BiPMValue = analogRead(phr1BiPMPin);
    phr2BiPMValue = analogRead(phr2BiPMPin);
    delay(shortDelay);
}

void bipolarMoveBackward() {
    while (phr2BiPMValue < phr1BiPMValue & stepCountBiPM >
stepBLimitBiPM) {
        biPStepper(-49);
        stepCountBiPM = stepCountBiPM - 49;

```

```

    delay(shortDelay);
}

while (sampleCount < numSamples) {
    sumPhr1BiPM += analogRead(phr1BiPMPin);
    sumPhr2BiPM += analogRead(phr2BiPMPin);
    sampleCount++;
    delay(shortDelay);
}

phr1BiPMValue = analogRead(phr1BiPMPin);
phr2BiPMValue = analogRead(phr2BiPMPin);
delay(shortDelay);
}

void sweep(){
if (stepCountUniPM >= 0 ){
    for (i = 0; i < stepCountUniPM; i++) {
        if (stepCountUniPM > stepBLimitUniPM){
            uniPStepper(-32);
            stepCountUniPM = stepCountUniPM - 32;
            delay(shortDelay);
        }
    }
}
else {
    for (i = 0; i > stepCountUniPM; i++) {
        if (stepCountUniPM < stepFLimitUniPM){
            uniPStepper(32);
            stepCountUniPM = stepCountUniPM + 32;
            delay(shortDelay);
        }
    }
}
}
}

```

Univerzita Hradec Králové  
Faculty of Informatics and Management  
Academic Year: 2016/2017  
Obor v rámci kterého má být VŠKP vypracována: Information Systems Management

Study Programme: Systems Engineering and Informatics  
Form: Full-time  
Branch/comb.: Informační management (im3-p-an)

**Document for registration BACHELOR STUDENT'S THESIS**

<b>Submits:</b>	<b>ADDRESS</b>	<b>PERSONAL NUMBER</b>
Bayat Mina	Bigdeli Dead-endShariati Ave., Tehran Building 94, Tehran	I14830

**TOPIC IN CZECH:**

Optimalizace výkonu solárního panelu pomocí smart hardware

**TOPIC IN ENGLISH:**

Optimization the power output of solar panel using smart hardware

**SUPERVISOR:**

Ing. Jan Štěpán - KIT

**RESEARCH PLAN:**

1. Title Page
2. Declaration
3. Acknowledgements
4. Abstract (Czech and English)
5. Contents
6. Introduction
7. Literature Search
8. Project Objectives, Choice of Methodology and Solution Description
9. Main Chapters
10. Results
11. Conclusions and Recommendations
12. Bibliography
13. Appendix

**List of recommended literature:**

1. Purdum, J. (2015). Beginning C for Arduino: Learn C Programming for the Arduino. Apress. ISBN 978-1-4842-0941-7.
2. Brynjolfsson, E. & McAfee A. (2016). The Second Machine Age: Work, Progress, and Prosperity in a Time of Brilliant Technologies. W. W. Norton & Company. ISBN 0393350649.
3. Townsend, K. (Ed.). (2014). Getting Started with Bluetooth Low Energy: Tools and Techniques for Low-Power Networking. O'Reilly Media. ISBN 978-1-4919-4951-1.
4. Monk, S. (2016). Raspberry Pi Cookbook: Software and Hardware Problems and Solutions. O'Reilly Media. ISBN 978-1491939109.
5. Brian, W. K. (Ed.). (1988). The C Programming Language. Prentice Hall PTR. ISBN-13: 978-0131103627.
6. Boysen, E. (Ed.). (2012). Complete Electronics Self-Teaching Guide with Projects. Wiley. Ebook ISBN: 978-1-4571-4536-0.
7. Scarpino, M. (2015). Motors for Makers: A Guide to Steppers, Servos, and Other Electrical Machines. Pearson Education. ISBN 9780134032832.
8. Dunlop, J. P. In partnership with NJATC. (2009). Photovoltaic Systems Engineering. Amer Technical Pub. ISBN-13: 978-0826913081.

Student's signature: mina Beyast  
Supervisor's signature: shar

Date: 31.10.2016  
Date: 31.10.2016